AGU PUBLICATIONS

Geochemistry, Geophysics, Geosystems

RESEARCH ARTICLE
10.1002/2015GC005752

Profiling planktonic foraminiferal crust formation

Juliane Steinhardt[1], Lennart L. J. de Nooijer[1], Geert-Jan Brummer[1,2], and Gert-Jan Reichart[1,3]

[1]Department of Geology and Chemical Oceanography, The Royal Netherlands Institute for Sea Research, Texel, Netherlands, [2]Faculty of Earth- and Life Sciences, VU University Amsterdam, Amsterdam, Netherlands, [3]Department of Earth Sciences, Faculty of Geosciences, Utrecht University, Utrecht, Netherlands

Key Points:
- Mg/Ca is lower in the crusts and cortex compared to lamellar calcite
- Crust thickness and Mg/Ca decreases toward the younger chambers in *N. dutertrei*
- We present a depth-resolved model explaining crust and cortex formation

Supporting Information:
- Supporting Information S1

Correspondence to:
J. Steinhardt,
juliane.steinhardt@nioz.nl

Citation:
Steinhardt, J., L. L. J. de Nooijer, G.-J. Brummer, and G.-J. Reichart (2015), Profiling planktonic foraminiferal crust formation, *Geochem. Geophys. Geosyst.*, *16*, 2409–2430, doi:10.1002/2015GC005752.

Received 29 JAN 2015
Accepted 3 JUL 2015
Accepted article online 14 JUL 2015
Published online 26 JUL 2015

Abstract Planktonic foraminifera migrate vertically through the water column during their life, thereby growing and calcifying over a range of depth-associated conditions. Some species form a calcite veneer, crust, or cortex at the end of their lifecycle. This additional calcite layer may vary in structure, composition, and thickness, potentially accounting for most of their total shell mass and thereby dominating the element and isotope signature of the whole shell. Here we apply laser ablation ICP-MS depth profiling to assess variability in thickness and Mg/Ca composition of shell walls of three encrusting species derived from sediment traps. Compositionally, Mg/Ca is significantly lower in the crusts of *Neogloboquadrina dutertrei* and *Globorotalia scitula*, as well as in the cortex of *Pulleniatina obliquiloculata*, independent of the species-specific Mg/Ca of their lamellar calcite shell. Wall thickness accounts for nearly half of the total thickness in both crustal species and nearly a third in cortical *P. obliquiloculata*, regardless of their initial shell wall thickness. Crust thickness and crustal Mg/Ca decreases toward the younger chambers in *N. dutertrei* and to a lesser extent, also in *G. scitula*. In contrast, the cortex of *P. obliquiloculata* shows a nearly constant thickness and uniform Mg/Ca through the complete chamber wall. Patterns in thickness and Mg/Ca of the crust indicate that temperature is not the dominant factor controlling crust formation. Instead, we present a depth-resolved model explaining compositional differences within individuals and between successive chambers as well as compositional heterogeneity of the crust and lamellar calcite in all three species studied here.

1. Introduction

Planktonic foraminifera form calcite shells, which they extend step-wise by adding new chambers. Construction of these chambers follows a logarithmic spire in a tightly controlled building plan. Layers of primary and secondary calcite, together called the "lamellar" or "ontogenetic" calcite [*Reiss*, 1957, 1959, 1960; *Erez*, 2003] are formed with each chamber added. The secondary calcite, moreover, covers all preceding chambers of the last whorl during addition of every new chamber [e.g., *Reiss*, 1959, 1960; *Takayanagi et al*., 1968]. In various species, a final calcite layer with a markedly different morphology and thickness covers this lamellar calcite. Crusts, for example formed by blocky euhedral crystals, thicken the shell, reduce its porosity and give the surface of the chambers a rough appearance. Gametogenic calcite, in contrast, precipitates as a relatively thin veneer, giving spinose species in life a nonspinose appearance in the sediment [*Bé*, 1980; *Hemleben et al*., 1985]. Some foraminiferal species develop a thick final cortex of smooth glossy calcite [e.g., *Burt and Scott*, 1975; *Erez and Honjo*, 1981; *Kunioka et al*., 2006]. All are shell features that typically occur last in ontogeny, defined by *Brummer et al*. [1987] as the terminal stage of shell development associated with the reproductive process. However, unlike gametogenic calcite, there are no direct observations confirming the relation between reproduction and the construction of a crust or cortex.

Fossil tests of calcifying foraminifera are popular tools used to reconstruct marine environmental conditions and past climate change. Elemental and isotopic compositions of foraminiferal calcite depend on various environmental parameters such as temperature, salinity, pH, and ion concentration [*McCrea*, 1950; *Epstein et al*., 1951; *Boyle*, 1981; *Nürnberg et al*., 1996; *Lea et al*., 1999; *Russell*, 2004; *Dissard et al*., 2010; *De Nooijer et al*., 2014]. However, minor and trace elements are known to be distributed heterogeneously within foraminiferal tests [*Eggins et al*., 2003; *Hathorne et al*., 2003; *Allison and Austin*, 2003; *Sadekov et al*., 2005; *Kunioka et al*., 2006; *Jonkers et al*., 2012]. This is mainly caused by physiological (i.e., biomineralization) controls on chamber formation [*Bé*, 1960; *Hemleben et al*., 1989; *Fairbanks et al*., 1980; *Erez*, 2003; *De Nooijer et al*., 2009; *Steinhardt et al*., 2014; *Vetter et al*., 2014], although the absolute values may be modified by depth migration

during their life cycle. Diurnal rhythms in symbiont activity potentially cause the alternating bands of high-Mg/Ca and low-Mg/Ca ratios found in some species [*Bemis et al*., 2000; *Eggins et al*., 2004; *Spero et al*., 2015]. Also calcification features such as crust and cortex calcite introduce potential sources of within-specimen and between-specimen variability in calcite chemistry of many planktonic foraminifera. Not only differences in chemical composition, but also relative contributions from the different calcite layers [*Takayanagi et al*., 1968] may affect average whole shell composition on which temperature calibrations are currently based [e.g., *Dekens et al*., 2002; *Anand et al*., 2003; *Cléroux et al*., 2008; *Regenberg et al*., 2009].

Here we investigate the thickness and composition of crust calcite, whether it differs chemically and morphologically from a cortex and assess how their formation is linked to the foraminiferal life cycle. For this purpose, we selected specimens from three planktonic foraminiferal species with contrasting life cycles, all known to form crusts or a cortex. *Neogloboquadrina dutertrei* is a mixed layer dweller, *Pulleniatina obliquiloculata* has a similar albeit somewhat deeper assumed habitat, and *Globorotalia scitula* is a subsurface to deep dwelling species [e.g., *Bé and Hutson*, 1977; *Fairbanks et al*., 1982; *Watkins et al*., 1996; *Ortiz et al*., 1996; *Mücke and Oberhänsli*, 1999; *Steinhardt et al*., 2014]. We compare structural differences between lamellar, crust, and cortex calcite using SEM imaging in combination with laser ablation (LA) ICP-MS depth profiling of shell walls to investigate compositional differences within and between species and to quantify their contribution to the overall calcite composition. Quantifying the impact of environmental parameters on the incorporation of elements and isotopic fractionation allows improving proxies for downcore reconstructions [e.g., *Fischer and Wefer*, 1999; *Henderson*, 2002; *Zeebe et al*., 2008; *Katz et al*., 2010]. Hence, understanding the fundamental processes underlying crust and cortex formation sets the stage for further refinement of foraminiferal shell chemistry-based proxies.

2. Material and Methods

2.1. Species Selection and Chambers Analyzed

In this study we used material collected with a Technicap PPS 5 sediment trap (supporting information Table S1) that was deployed at 16.8°S and 40.8°E in the central Mozambique Channel (MC). The trap was positioned 250 meters above the channel floor, at water depth of 2250 m. Sea surface temperatures (SST) in the MC vary seasonally (ranging from 25°C to over 30°C with an annual mean of 27.6°C). Sea surface salinities decrease slightly from 35.2 in winter to 34.9 in summer [*Fallet et al*., 2010].

Processing of the time-series sediment trap samples is described in *Fallet et al*. [2009; 2010]. We selected three planktonic foraminiferal species, known to add either crust calcite or form a cortex layer. These species dwell at different times and at different depth intervals in the water column [e.g., *Erez and Honjo*, 1981; *Wilke et al*., 2006; *Jonkers et al*., 2012; *Steinhardt et al*., 2014]. Subsurface-dwellers *N. dutertrei* and *P. obliquiloculata* have been suggested to calcify between 0 and 100 m depth and between 60 and 150 m, i.e., in the upper and middle seasonal thermocline, respectively [*Cléroux et al*., 2007; *Erez and Honjo*, 1981; *Fairbanks et al*., 1982; *Field*, 2004; *Huang et al*., 2008; *Kuroyanagi and Kawahata*, 2004; *Pflaumann and Jian*, 1999; *Ravelo and Fairbanks*, 1992; *Spero et al*., 2003]. We also selected specimens of the deep-dwelling *G. scitula* to analyze the impact of deeper, colder waters on the thickness and composition of crusts [*Bé*, 1969; *Ortiz et al*., 1996; *Fallet et al*., 2011; *Itou et al*., 2001]. A depth habitat within the upper 1000 m has been suggested for this species [*Schiebel et al*., 1995; *Ortiz et al*., 1996; *Itou et al*., 2001]. Together, these three foraminiferal species cover a major part of the upper water column at a single location and hence encompass a major temperature range.

Specimens were selected from the >315 μm size fraction as much as possible to ensure the selection of mature specimens. In case insufficient specimens from the designated trap samples (supporting information Table S1) were available within this size range for replicate LA-ICP-MS analyses, specimens in the 250–315 μm were added to the pool of analyzed specimens (supporting information Table S2). We measured thickness and elemental composition of the final three to four chambers as these are positioned in the final whorl in all three species studied.

2.2. LA-ICP-MS

The Mg/Ca ratios of single chambers used in this study were previously published [*Steinhardt et al*., 2014] and were determined by Laser Ablation-Inductively Coupled Plasma-Mass Spectrometry (LA-ICP-MS) at

Utrecht University [*Reichart et al.*, 2003]. The matrix matched in-house standard showed an average relative standard deviation (SD) for Mg/Ca of 3.7%. Measurements were performed on intact specimens and always proceeded from the outside toward the inside of the chambers.

In addition to these laser ablation analyses, we added high-resolution profiles by ablating 12 specimens per species with a NWR193UC (New Wave Research) using an ArF Excimer laser (193 nm) with short pulse (<4 ns) and a dual volume TruLine cell with fast (<1 s) wash out time. Ablation was performed at a repetition rate of 4 Hz with an energy density of 1 Jcm^{-2} using an 80 μm, circular diameter spot size. The aerosol was transported out of the cell with a helium flow rate of 0.8 L/min of cell gas and 0.3 L/min of cup gas to a quadrupole ICP-MS (Thermo Scientific iCAP-Q). Foraminiferal shells were typically ablated from the outside toward the inside of the chambers. A signal-smoothing device between the cell and the ICP-MS was used to improve ratio stability [e.g., *Tunheng and Hirata*, 2004; *Evans and Müller*, 2013]. To optimize sensitivity and minimize ThO^+/Th^+, 0.3 mL/min Ar gas was admixed to the He flow before being introduced into the plasma. To minimize cycle time between masses and hence improve depth resolution, only four masses were measured: ^{24}Mg, ^{27}Al, ^{43}Ca, and ^{238}U. ThO^+/Th^+ ratios were maintained at levels between 0.1 and 0.7%. Concentrations of Mg and confidence intervals for each individual ablation profile were calculated using Thermo Qtegra software (version 2.2.1465.44) and ablation of an SRM NIST610 standard every 10 samples. The matrix matched in-house standard showed an average relative standard deviation (RSD) for Mg/Ca of 2.7%. In total, 629 single-chamber profiles were obtained. Crust and cortex Mg concentrations are based on the low Mg/Ca part at the beginning of the ablation profiles, whereas lamellar calcite is based on the integration over the higher Mg/Ca part of the ablation profile. The boundary between the crust (or cortex) and lamellar calcite is not always marked by an instantaneous change in Mg/Ca and therefore, the precise location of the boundary between crust and lamellar calcite can be placed within error limits. However, ablation profiles in this study are generally relatively long and shifting the boundary by a few seconds does therefore not have a noticeable impact on the average crust/cortex and lamellar Mg/Ca ratios. Regardless of the spatial resolution, profiles measured both with the LA-Sector Field-ICP-MS and that measured with the LA-Quadrupole-ICP-MS show similar thickness of low-Mg and high-Mg parts of crust or cortex and lamellar calcite. Previously measured LA-Sector Field-ICP-MS profiles [*Steinhardt et al.*, 2014, Figure 4] are as representative as LA-Quadrupole-ICP-MS ablation profiles. Profiles showing concentrations deviates more than twice the standard deviation from the average of the initial data set were regarded outliers and therefore discarded from the data set (28 from the 629).

2.3. Embedding, Etching, and Scanning Electron Microscopy (SEM)

A minimum of 12 specimens of each species were dissected after laser ablation by breaking off the ablated chambers individually with a fine needle. All SEM pictures were taken with a Hitachi High-Tech TM3000 tabletop microscope, allowing measurement of the wall thickness of the ablated specimens. Each chamber wall was vertically positioned on a carbon stub, so that the chamber cross-section was positioned perpendicularly to the SEM's electron beam. Using the machine's software, thicknesses of the crust, lamellar calcite, and the complete chamber wall were determined (Figure 1).

2.4. Electron Microprobe

To cross-validate element profiles obtained by LA-ICP-MS to determine thickness of crust and lamellar calcite, element maps were made using electron microprobe. We embedded nine specimens of each species in resin (Araldite 20/20). After 24 h, after the resin was fully hardened, a thin layer of the resin's surface was removed by sanding paper to expose a cross section of the foraminiferal specimens. The samples were rinsed thoroughly with distilled water and subsequently polished with increasingly finer sanding. After rinsing again with distilled water and drying, the surface was etched with 0.5% hydrochloric acid for approximately 5 s. The etched surface was rinsed again with distilled water and left to dry at 50°C. These etched samples allow for detection of the position of the primary organic template and measurement of the thickness of the crust versus that of the lamellar calcite using electron microprobe mapping. A number of polished cross-sectioned *P. obliquiloculata* specimens were not etched but carbon coated and placed in the electron microprobe (JEOL JXA-8530FField emission Electron Probe Micro Analyzer) for mapping Mg and Ca at 15kV. Mapping of the entire specimen was carried out in lower spatial resolution, using a dwell time of 500 ms, a spot diameter of 2 μm, and a step size of 2 μm (image: 320 $\times$ 320 points). Subsequently, on the same specimen, selected sections of the F-0 and F-2 chamber walls were mapped at higher resolution

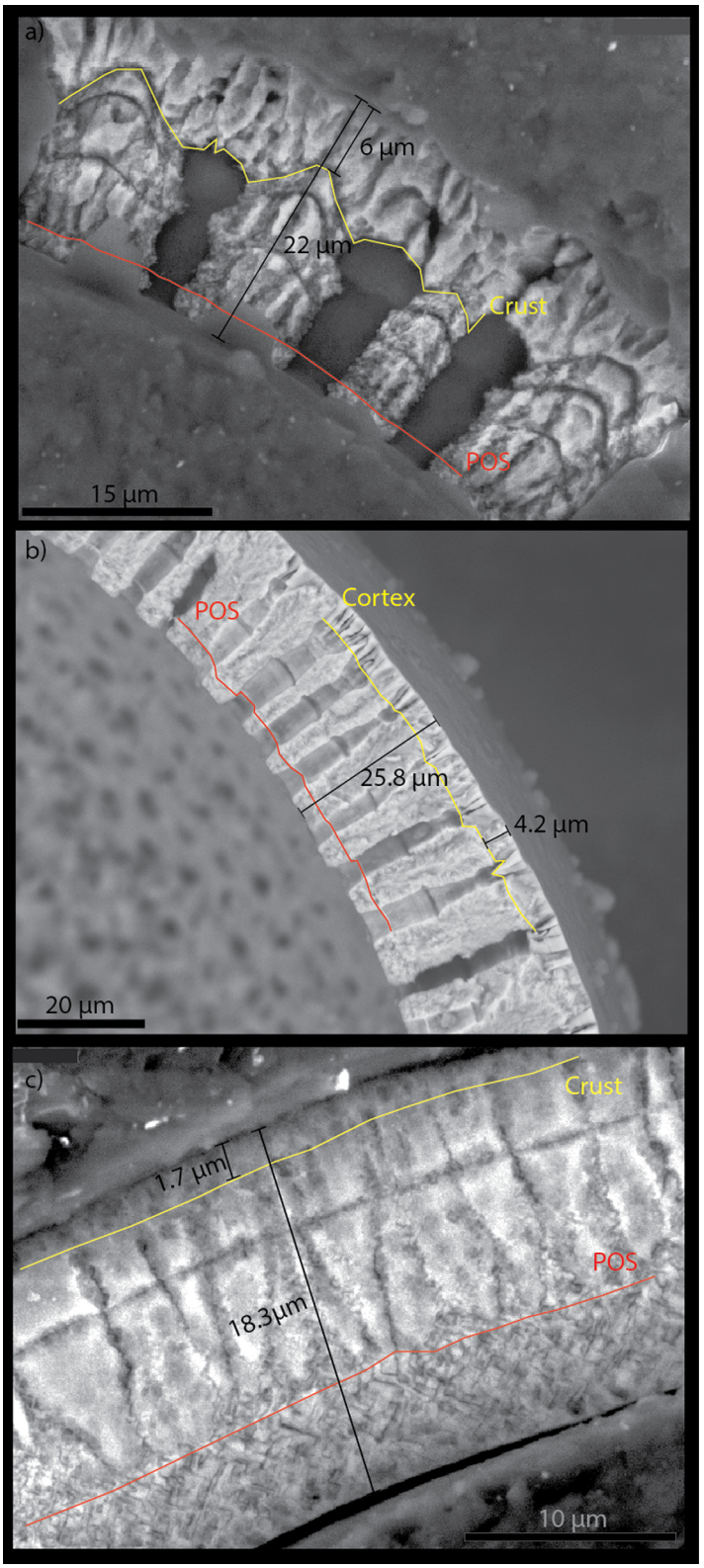

Figure 1. SEM image of chamber wall cross section of different species of planktonic foraminifera. Red line indicates the location of the POS, yellow line, cortex/crust, and black line indicates chamber wall thickness and crust/cortex thickness. (a) Cross-section image of an F-2 chamber wall of *N. dutertrei* (b) Cross-section image of an F-1 chamber wall of *P. obliquiloculata*. Note how the cortex is covering the pore space (c) Cross-section image of an F-1 chamber wall of *G. scitula*.

(images: 200 × 200 points) using a dwell time of 1000 ms, a spot diameter of 1 μm, and a 0.5 μm step size. Counts (current strength) were converted to elemental ratios by combining the maps by using forsterite as standard for Mg and diopside for Ca concentrations.

3. Results

3.1. Crust and Cortex Distribution

Crust and cortex are visually clearly distinct in SEM images of cross-sectioned walls (Figure 1). Also the embedded shells, upon etching, show a clear separation between lamellar and crust and/or cortex calcites (Figure 2). These images hence allow measuring thicknesses of the lamellar and crust calcites. Wall thickness (in micrometer) and number of laser pulses needed to ablate through the test wall are positively correlated ($r^2 = 0.59$; Figure 3) at approximately 40 nm per pulse (Figure 3). This rate is, considering the energy density used (1 Jcm^{-2}), in line with earlier reported rates of 150 nm/pulse at 5 Jcm^{-2} [*Eggins et al*., 2003] and 200–300 nm/pulse at 10 Jcm^{-2} [*Reichart et al*., 2003]. Moreover, Mg/Ca ablation profiles fitted the visual properties of crust/cortex and lamellar calcite (Figures 2a–2c). The smooth cortex of *P. obliquiloculata* can be clearly differentiated from the crust in e.g., *N. dutertrei*, as it does not show larger-sized euhedral crystals on its surface, and lacks pustule-like structures except around its aperture (Figures 4a–4d).

Based on the geochemistry of the ablation profiles and SEM shell thickness measurements, the crust contributes approximately half (7.6 ± 0.5 μm or ±47%) to the total thickness of chamber walls of *N. dutertrei* (16.2±4.2 μm). There is a significant difference in crust thickness between chambers within specimens of *N. dutertrei* (Figure 5a). To compare the different shell chambers, we labeled successive chambers from the chamber added last (F-0) toward earlier formed chambers using the preceding position with respect to this first chamber, with n counting back along the whorl (F-n). Also lamellar calcite increases significantly in thickness between F-0 and F-2 (Jonckheere-Terpstra test, $p = 0.002$) and between F-0 and F-3 (Jonckheere-Terpstra test, $p < 0.0001$), as well as the F-1 and F-3 (Jonckheere-Terpstra test, $p = 0.018$). In *P. obliquiloculata*, cortex (7.1 ± 0.3 μm) contributes on average 32% to the total wall thickness (24.0 ± 5.3 μm) and is remarkably similar in successive chambers (Figure 5b) as is the thickness of its lamellar calcite (Table 1). Lamellar calcite in *G. scitula* shows a gradual, but significant, increase in thickness from the youngest toward the older chambers (Figure 5c). In *G. scitula*, the crust (7.2 ± 0.4 μm) contributes on average 45.6% to the total wall thickness (15.8 ± 3.2 μm) and, albeit with some variability, does not change significantly between successive chambers (Figure 5c).

3.2. Crust, Cortex and Lamellar Mg/Ca

Combined analysis on the same specimen show that low Mg/Ca ratios from LA-ICP-MS analyses correlate well with visually identified crust for *N. dutertrei* and *G. scitula* and cortex for *P. obliquiloculata* morphology in all three species (Figures 6a–6f). This correlation is confirmed by Electron Microprobe element maps of cross-sectioned shells (Figure 7) clearly showing lower Mg/Ca ratios in that part of the outer wall corresponding to the cortex. The difference in Mg/Ca between the outer crust/cortex and the inner lamellar calcite hence allows determining absence/presence of crusts and/or cortex and when present, its thickness (Figures 7a–7c). Accordingly, we identified low Mg/Ca crusts in 60% (N = 164) of the chambers in the final whorl of *G. scitula*, 70% (N = 335) in those of *N. dutertrei* and up to 93% (N = 109) in the cortex of *P. obliquiloculata* chambers. On average, the Mg/Ca of the lamellar calcite was similar between specimens with and without a crust (Figure 8a). However, the Mg/Ca of the crusts is considerably lower than that of the lamellar calcite for all three species (Figure 8b). In *N. dutertrei*, average crust Mg/Ca was 1.83 ± 0.79 mmol/mol (N = 223, SE: ±0.05 mmol/mol), which was significantly lower (Mann-Whitney test, $p < 0.001$) than Mg/Ca for the lamellar calcite (3.22 ± 0.99 mmol/mol; N = 344, SE: ±0.06 mmol/mol) (Figure 8b). For *P. obliquiloculata* cortex, Mg/Ca values are on average 1.17 ± 0.41 mmol/mol (N = 107, SE: ±0.04 mmol/mol), compared to 2.86 ± 0.81 mmol/mol for the lamellar calcite (N = 113, SE: ±0.08 mmol/mol), a significant difference according to the Mann-Whitney test ($p < 0.001$). The Mann-Whitney test is a nonparametric test of the null hypothesis that compares two unpaired groups from the same population, with a particular population tending to have larger values than the other [e.g., *Mann and Whitney*, 1947; *Ramsey*, 2000]. Crust Mg/Ca values for *G. scitula* are on average 0.93 ± 0.35 mmol/mol (N = 97, SE: ±0.04 mmol/mol), which is significantly lower (Mann-Whitney test, $p = 0.006$) than in the lamellar calcite (1.60 ± 0.45 mmol/mol, N = 164, SE: ±0.04 mmol/mol).

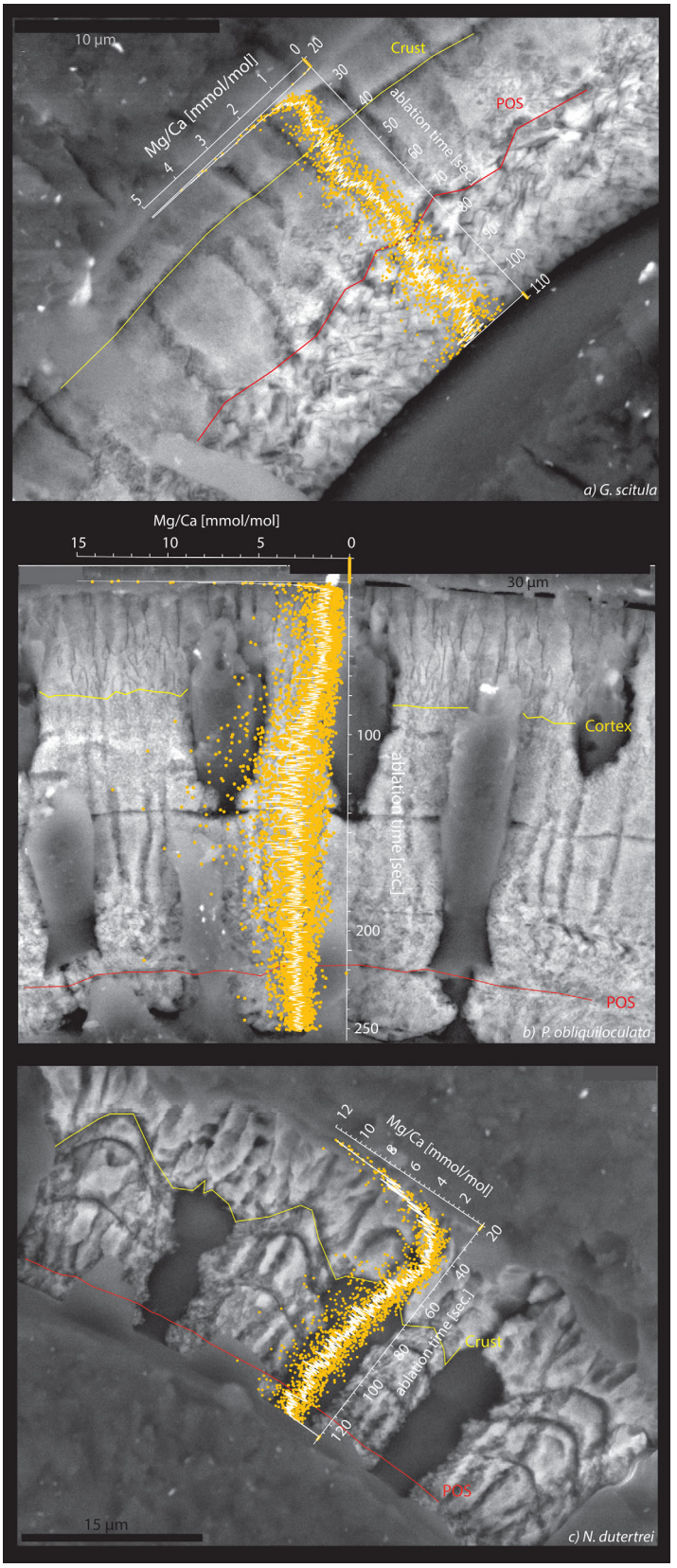

Figure 2. SEM images of an embedded polished and etched specimen of (a) *G. scitula*, (b) *P. obliquiloculata*, and (c) *N. dutertrei*. The chamber cross-section images are overlaid with the matching LA-ICP-MS Mg/Ca profiles from the same chamber.

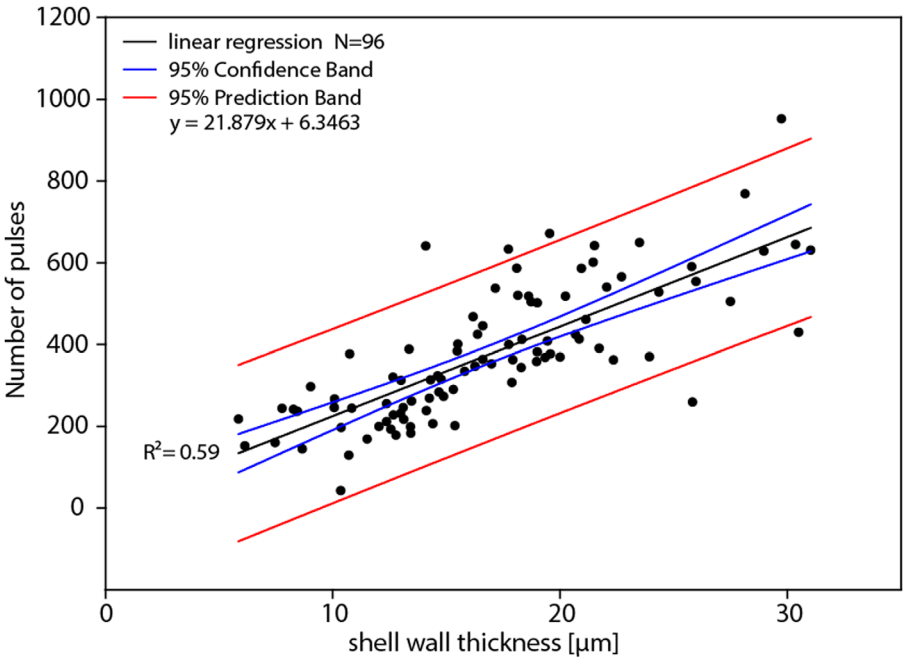

Figure 3. Ablation length (in pulses) and wall thickness (in micrometer) are positively correlated in the 41 number of specimens analyzed of *N. dutertrei*, *P. obliquiloculata*, and *G. scitula*.

No significant variation in average Mg/Ca between successive chambers is detected in the cortex of *P. obliquiloculata* and crust of *G. scitula* (Figure 9), nor in the lamellar calcite of *G. scitula*. However, Mg/Ca of the lamellar calcite of *P. obliquiloculata* does show significant differences between chambers (One way Anova, $p = 0.018$), i.e., between the final (F-0) and penultimate (F-1) chamber (pairwise multiple comparison Holm-Sidak method following the one way ANOVA, $p = 0.047$) and also between F-0 and the prepenultimate (F-2) chamber ($p = 0.033$). Similarly, in *N. dutertrei* we observed a significant difference between the Mg/Ca of the crust in F-0 (Mg/Ca: 2.48 ± 0.79 mmol/mol, SE: ±0.12 mmol/mol) and F-1 (Mg/Ca: 1.87 ± 0.76 mmol/mol, SE: ±0.08 mmol/mol) (Figure 9; Mann-Whitney test, $p < 0.001$) and also between crust calcite in F-1 and F-2 (Mg/Ca: 1.51 ± 0.62 mmol/mol, SE: ±0.07 mmol/mol) (Mann-Whitney test, $p = 0.009$). Differences between crust Mg/Ca values in F-2 and F-3 (1.54 ± 0.63 mmol/mol, SE: ±0.15 mmol/mol) are not significant. Furthermore, lamellar Mg/Ca for *N. dutertrei* significantly differs between F-0 (Mg/Ca: 3.61 ± 1.10 mmol/mol, SE: ±0.12 mmol/mol) and F-1 (Mg/Ca: 3.12 ± 0.91 mmol/mol, SE: ±0.08 mmol/mol) and between the F-0 and F-2 chambers (Mann-Whitney test, $p < 0.001$).

4. Discussion

4.1. Constraints on Crust and Cortex Formation Based on Mg/Ca

In all species studied here, the element composition of crust and cortex calcite differs from that of the lamellar calcite, coinciding with morphological differences between the two types of calcite. In general, crust and cortex Mg/Ca are relatively low with minor variability within species, but varies significantly between species (One way ANOVA, $p < 0.001$). There are no significant changes in crust/cortex Mg/Ca between eddy and non-eddy intervals. Changes in crust/cortex and lamellar Mg/Ca are minor between eddy and non-eddy intervals and are negligible compared to differences in Mg/Ca between crust/cortex and lamellar calcite.

The offset between crust and lamellar calcite Mg/Ca (Figures 2c and 8b) is in line with earlier studies showing lower values in crusts of *G. truncatulinoides* [*Duckworth*, 1977], *G. inflata* [*Van Raden et al*., 2011], and *N. dutertrei* [*Eggins et al*., 2003; *Jonkers et al*., 2012]. These earlier studies related the low crust Mg/Ca primarily to terminal calcification in deeper and hence colder waters. Irrespectively, the observed strong partitioning against seawater Mg indicates that crust and cortex calcification is even more strongly biologically controlled than that of the lamellar calcite. This contrasts with the markedly higher Mg/Ca values of diagenetic

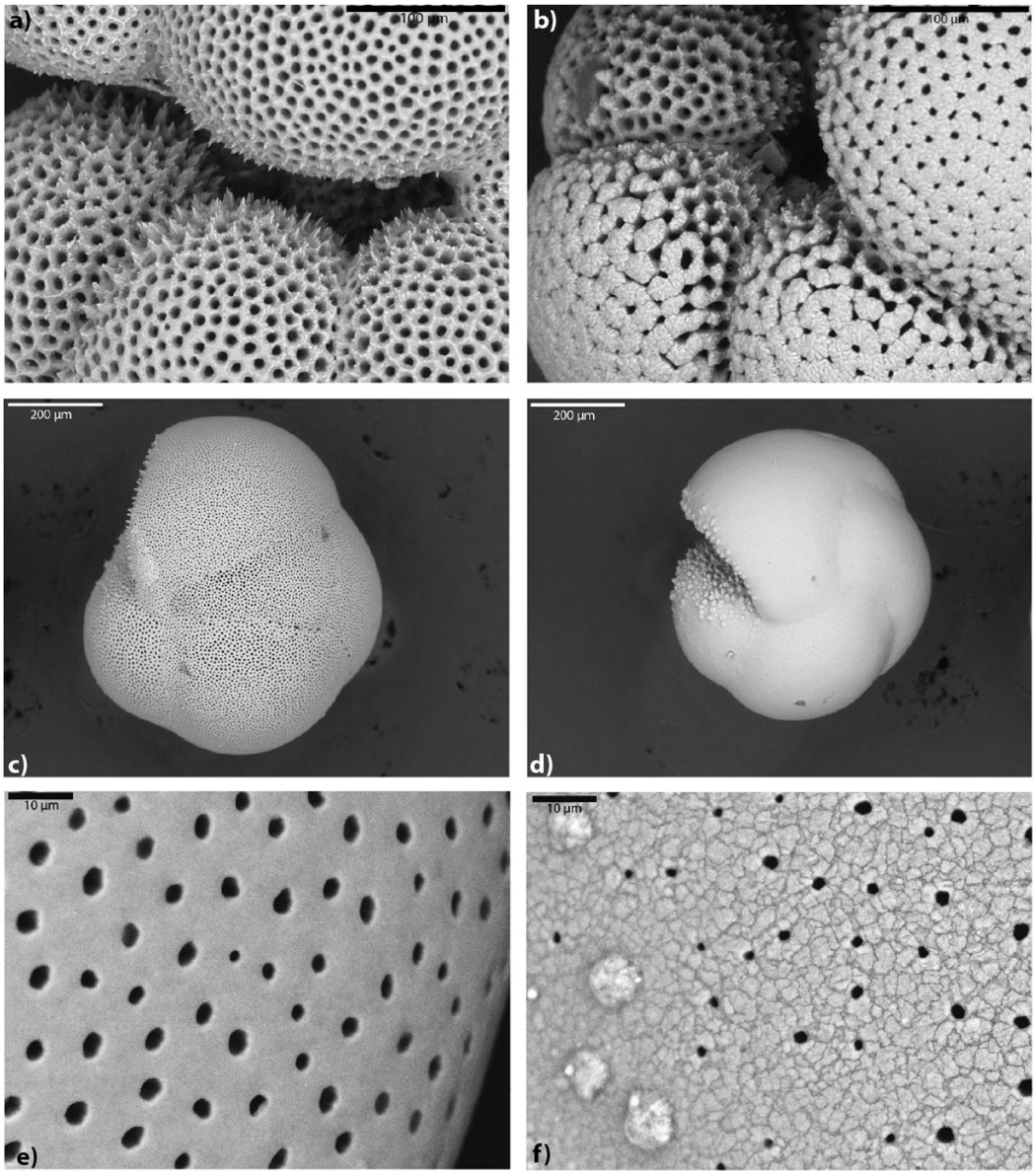

Figure 4. SEM images of encrusted (left) and non-encrusted (right) planktonic foraminifera. (a) Nonencrusted shell surface of *N. dutertrei* (b) encrusted *N. dutertrei* (c) *P. obliquiloculata* with early cortex, (d) cortex covered *P. obliquiloculata*, (e) nonencrusted shell surface of *G. scitula*, and (f) encrusted shell surface of *G. scitula*.

calcite precipitated after burial in the sediment [*Pena et al*., 2005]. Since the foraminiferal shells studied here are retrieved from sediment traps, neither diagenetic crust is expected, nor did inorganic calcite precipitate on the shells while settling through the water column.

A pairwise multiple comparison using the Dunn's Method, testing for stochastic dominance and reports the results among multiple pairwise comparisons after a Kruskal-Wallis test for stochastic dominance among different groups [*Kruskal and Wallis*, 1952], showed that all three species differ significantly in crust/cortex Mg/Ca from each other. Of all species studied here, the crust of *N. dutertrei* has highest Mg/Ca values, whereas crust Mg/Ca values for *P. obliquiloculata* and *G. scitula* are relatively low. Higher crustal Mg/Ca values for *N. dutertrei* are in line with its overall shallower habitat compared to that of the other species investigated in this study. However, similar Mg/Ca values of the crust in *G. scitula* and cortex in *P. obliquiloculata* conflict with their contrasting temperature-derived depth habitats [*Steinhardt et al*., 2014]. This difference in Mg/Ca despite precipitation at similar temperatures or depths, suggests that biological fractionation is overprinting

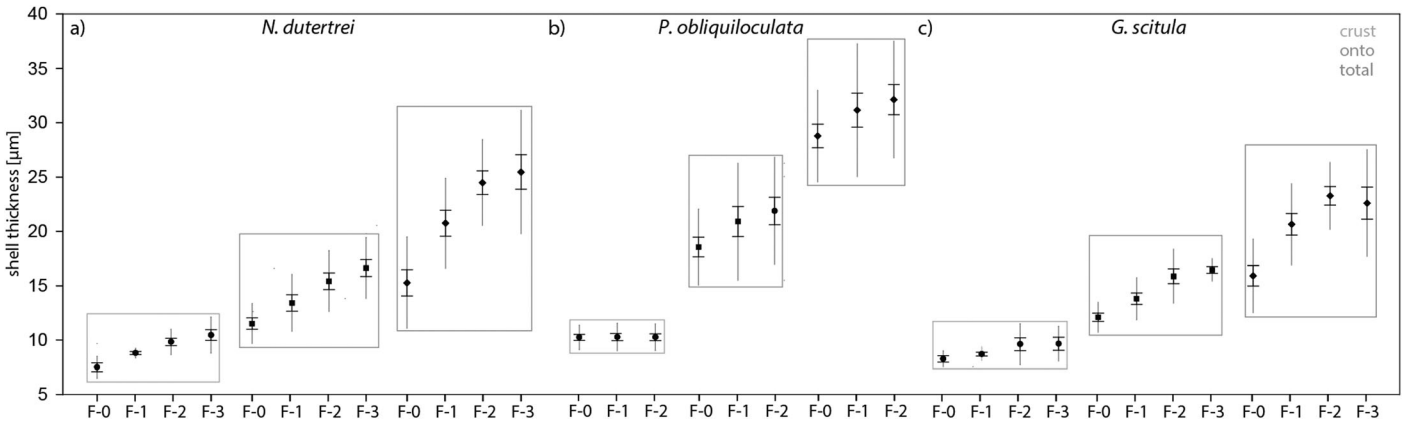

Figure 5. Wall thickness of several chambers of *N. dutertrei*, *P. obliquiloculata*, and *G. scitula*. Average shell thickness of crust, lamellar, and total shell calcite are indicated by circles. Error bars indicate standard error, extended grey lines show standard deviations (D, 1 sigma).

the effect of depth-induced temperature decrease on crust/cortex chemistry. This implies that the difference in Mg/Ca between lamellar and crust/cortex calcite not solely depends on depth habitat-related temperature changes.

The largest difference in average Mg/Ca between crust and lamellar calcite is found in *P. obliquiloculata* (ΔMg/Ca$=$ 1.74 $\pm$ 0.08 mmol/mol), slightly less in *N. dutertrei* (ΔMg/Ca $=$ 1.64 $\pm$ 0.08 mmol/mol), and smallest in *G. scitula* (ΔMg/Ca: 0.71 $\pm$ 0.05 mmol/mol). Translated into temperatures using species-specific calibrations [*Anand et al*., 2003], average lamellar calcite Mg/Ca values of *N. dutertrei* correspond to a temperature of 24.9°C, whereas its crust would reflect a temperature of 18.6°C. Likewise, *P. obliquiloculata*'s average lamellar Mg/Ca suggest a calcification temperature of 24.1°C, whereas its crustal Mg/Ca (Figure 8b) yields a temperature of 14.1°C, corresponding to depths around 60 and 310 m in the Mozambique Channel, respectively. The integrated, average wall Mg/Ca (2.4 mmol/mol) translates into a temperature of 22°C, found at a depth of approximately 100 m. Average lamellar calcite Mg/Ca values of *G. scitula* correspond to a temperature of 15.2°C, whereas average crust Mg/Ca reflect a temperature of 9.1°C, indicating calcification at 250 and 620 m, respectively. Average wall Mg/Ca (1.48 mmol/mol) translates into a temperature of 14.3°C, at approximately 290 m depth. For all these species, Mg/Ca-temperature reconstructions suggest a substantial deepening in habitat between lamellar calcite and crust/cortex formation. However, this assumes that calibrations based on multiple, whole shells [*Anand et al*., 2003] can be applied to individual layers within the shell wall, which is highly unlikely given the observed offset between lamellar and crust/cortex Mg/Ca. There are (at least) two processes responsible for the Mg/Ca difference within and between species: a biomineralization control and a habitat-related component that modifies the overall Mg/Ca (and possibly, its within-shell heterogeneity).

Interestingly we observe a gradient in crust Mg/Ca values of successive chambers in *N. dutertrei* (Figure 9), which is in line with earlier observations of *Jonkers et al*. [2012]. This implies that when crust formation is

Table 1. A Jonckheere-Terptra Test is a Nonparametric Test of Analysis of Variance Performed in SPSS (Version 20.0 for Windows, SPSS Inc., Chicago) to Test for Significant Trends in Mg/Ca and Shell Wall Thickness [*Lunneborg*, 2005][a]

	Mg/Ca			Thickness		
Species	Crust/Cortex	Onto	Average	Crust/Cortex	Onto	Average
N. dutertrei	*p* (2-tailed): 0.000, r (Pearson): −0.423[b]	*p* (2-tailed): 0.001, r (Pearson): −0.188[b]	*p* (2-tailed): 0.000, r (Pearson): −0.262[b]	*p* (2-tailed): 0.003, r (Pearson): 0.475[b]	*p* (2-tailed): 0.000, r (Pearson): 0.543[b]	*p* (2-tailed): 0.000, r (Pearson): 0.726[b]
P. obliquiloculata	*p* (2-tailed): 0.462	*p* (2-tailed): 0.013, r (Pearson): −0.221[c]	*p* (2-tailed): 0.137	*p* (2-tailed): 0.692	*p* (2-tailed): 0.054, r (Pearson): 0.278	*p* (2-tailed): 0.650
G. scitula	*p* (2-tailed): 0.971	*p* (2-tailed): 0.745	*p* (2-tailed): 0.122	*p* (2-tailed): 0.042, r (Pearson): 0.300[c]	*p* (2-tailed): 0.000, r (Pearson): 0.453[b]	*p* (2-tailed): 0.000, r (Pearson): 0.587[b]

[a]Results of this test for intraspecies trends in Mg/Ca and shell wall thicknesses reveal significant correlations at the 0.005 level (2-tailed) and significant correlations at the 0.001 level (2-tailed), indicated by a "b" and "c", respectively.
[b]Jonckheere-Terpstra test: correlation is significant at the 0.001 level (2-tailed).
[c]Jonckheere-Terpstra test: correlation is significant at the 0.005 level (2-tailed).

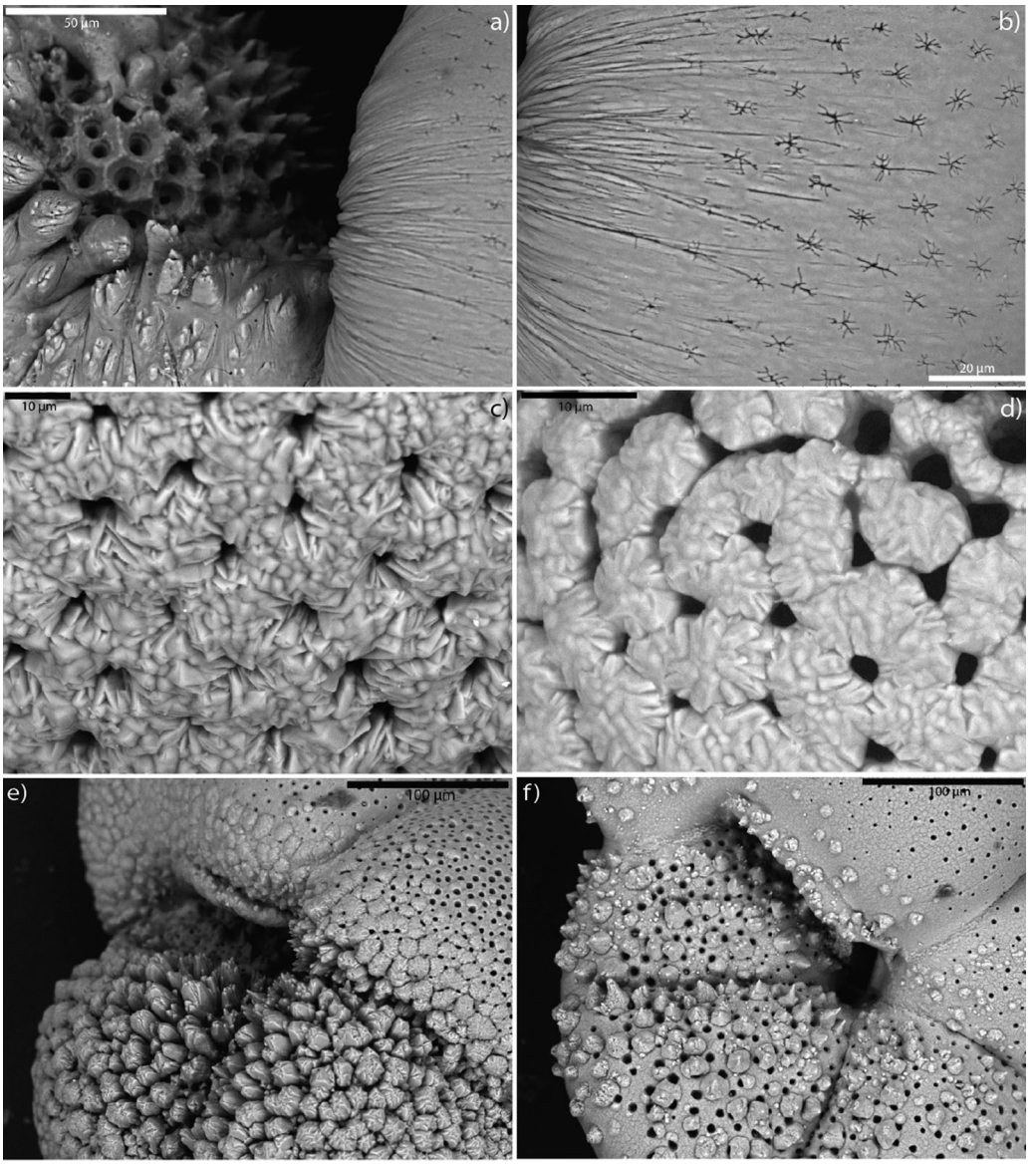

Figure 6. Crustal features of (a and b) *P. obliquiloculata*, SEM image showing details of the aperture. Visible stream marks (striae), emerging from the aperture, imprinted on the cortex. Markedly smaller pore openings (fissure-like) due to cortex cover. (c and d) *N. dutertrei* with euhedral crystals. (e and f) *G. scitula* crust crystals and pustules, which are isolated ornamentations on otherwise relatively smooth lamellar calcite.

indeed triggered by temperature, as suggested earlier by *Hemleben and Spindler* [1983], crust formation continued when temperatures decreased further. A change in metabolic rate, related to temperature could also cause an overall shift in the mode of calcification and result in a different partitioning for Mg (supporting information Figure S1). The Mg/Ca-derived temperature difference of the lamellar calcite between chamber F-0 and F-1 is 1.6°C, while Mg/Ca differences in their crust correspond to a temperature of 3.1°C. An integrated shell wall Mg/Ca average of 2.8 mmol/mol translates to a temperature of 23.3°C and a calcification depth of 75 m (supporting information Figure S1). Increased Mg/Ca in the crust of *N. dutertrei* could either indicate an increasingly warmer habitat during crust formation or a larger relative contribution of a high-magnesium phase. For gametogenic calcite, a thin terminal veneer precipitated immediately prior to gametogenesis in spinose planktonic foraminifers, *Nürnberg et al*. [1996] showed significantly enhanced Mg/Ca with respect to the lamellar calcite of *G. sacculifer* growing in culture. Since culture temperature was kept constant [*Nürnberg et al*., 1996], Mg/Ca partitioning in gametogenic calcite must be related to something other than temperature. Similar to our findings for *N. dutertrei*, *Jonkers et al*. [2012] also show

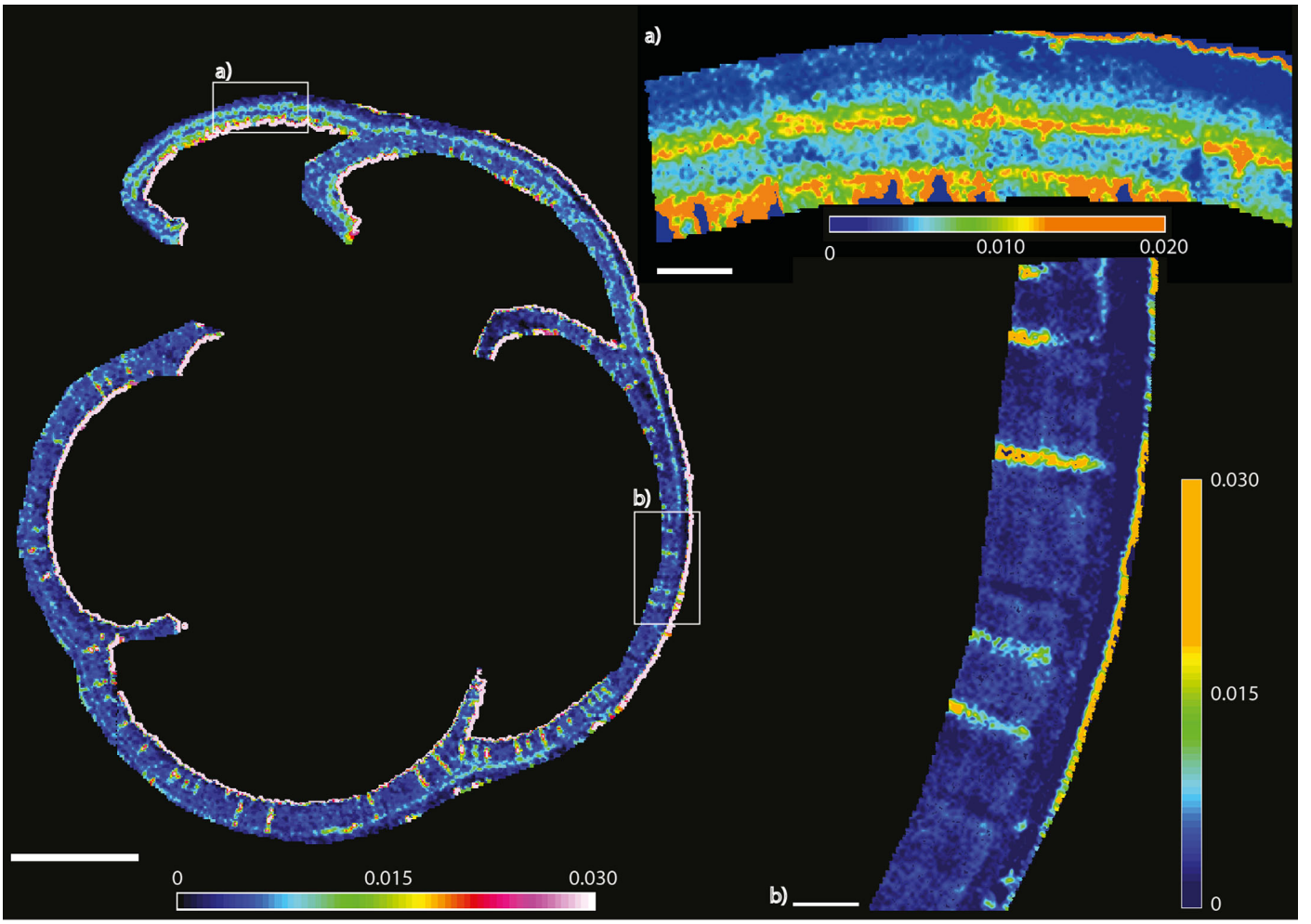

Figure 7. Mg/Ca (count ratios) distributions for a selected specimen of an encrusted *P. obliquiloculata* specimen. (a) Mg/Ca distribution map close-up of the F-0 chamber in high resolution (see 2.4 for method description) (b) Mg/Ca distribution map close-up of the F-2 chamber in high resolution (see 2.4 for method description). High Mg/Ca values at the edges and near pores are caused by irregularities at the shell-resin interface, the so-called edge effect [*Sadekov et al*., 2005; *Pena et al*., 2005; *Fehrenbacher and Martin*, 2010, 2014].

increasing crust Mg/Ca ratios toward the younger chambers, which is not in line with gradual habitat deepening alone. An increasing relative contribution of gametogenic calcite to the crust calcite could result in higher average Mg/Ca since the higher Mg concentrations in the gametogenic calcite increasingly affects the thinner crust toward the last chambers in *N. dutertrei*. However, gametogenic calcification only occurs last during ontogeny and ends the terminal stage, while crust formation in *N. dutertrei* appears a more prolonged process. Furthermore, as parent individuals do not survive gametogenesis (as observed in culture), crust/cortex cannot have formed after gametogenesis. Independent of the underlying mechanism, the observed gradient in crust Mg/Ca suggests that crust was sequentially added to the chambers during growth in *N. dutertrei*. This is in contrast to the two deeper dwelling species, which show similar Mg/Ca values for crust/cortex calcite in all chambers. Although this suggests similar depths for the entire crust/cortex of these two species, the relatively small temperature differences at larger depths might also obscure changes in depth habitat.

Inferred temperatures and calcification depths are only valid if Mg incorporation into crust/cortex and lamellar calcite follows the same temperature dependence within a species. However, microenvironmental controls related to foraminiferal physiology might result in disequilibrium fractionation [*De Nooijer et al*., 2014]. Reduced metabolic activity could hence impact partitioning during the terminal (reproductive) stage as opposed to the adult (growth) stage of the planktonic foraminiferal life cycle. The biological controls on element incorporation and isotope fractionation causing offsets between species are often summarized as "the vital effect" [*Urey et al*., 1951; *Weiner and Dove*, 2003]. These vital effects comprise (1) chemical alterations of the foraminiferal microenvironment by physiological processes, (2) cellular controls on the

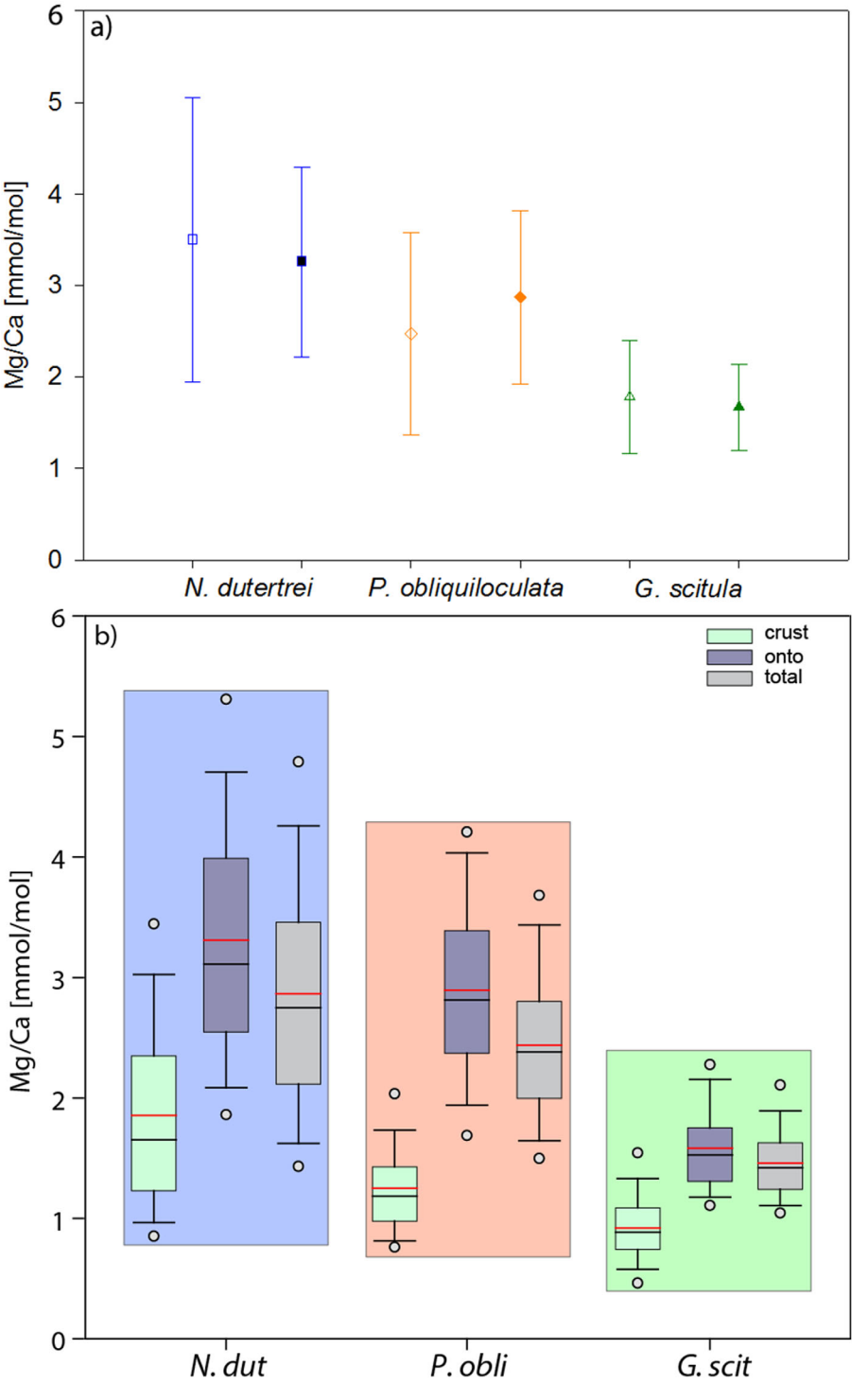

Figure 8. (a) Comparison of lamellar calcite of encrusted and nonencrusted specimens of *N. dutertrei*, *P. obliquiloculata*, *and G. scitula*. Open symbols indicate nonencrusted specimens, filled symbols encrusted specimens. (b) Box-plot of average crust, lamellar, and whole shell wall Mg/Ca for *G. scitula*, *P. obliquiloculata*, and *N. dutertrei*. In addition, the graph shows mean (red line) whereas the open circles indicate the 5th and 95th percentile. The Standard percentile method uses linear interpolation to determine the percentile values. The 50th percentile (median) is indicated with the black lines within the boxes. The open boxes are used to graphically show overall differences between species.

composition of the fluid from which calcite is precipitated, and (3) biological controls on crystal growth (e.g., via organic templates). Since these "vital effects" cause substantial species-specific offsets in Mg/Ca values [*Anand et al.*, 2003; *Bentov and Erez*, 2006; *Wit et al.*, 2010], they likely also produce a different,

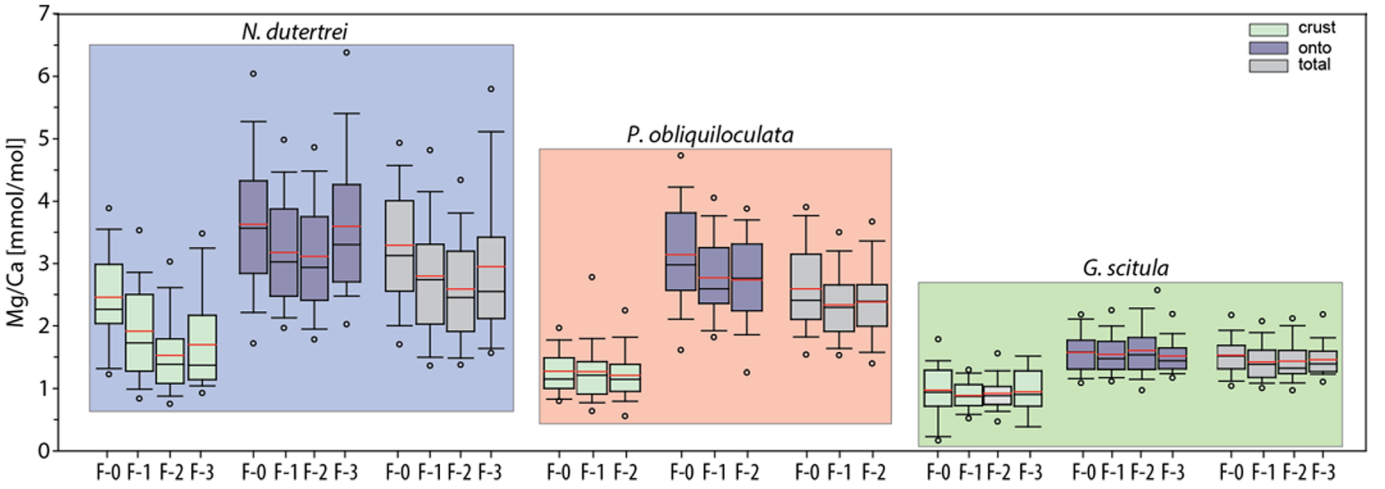

Figure 9. Box-plot of intratest variability of crust, lamellar, and total shell wall Mg/Ca for *G. scitula*, *P. obliquiloculata*, and *N. dutertrei*. The boundary of the box closest to zero indicates the 25th percentile, a line within the box marks the median, and the boundary of the box farthest from zero indicates the 75th percentile. Whiskers (error bars) above and below the box indicate the 90th and 10th percentiles. In addition, the graph shows mean (red line) whereas the open circles indicate the 5th and 95th percentile. The Standard percentile method uses linear interpolation to determine the percentile values. The 50th percentile (median) is indicated with the black lines within the boxes. The open boxes are used to graphically show overall differences between species.

ontogenetic partitioning between lamellar and crust/cortex calcite, e.g., as observed for the gametogenic calcite of *G. sacculifer* in temperature-controlled cultures [*Nürnberg et al*., 1996]. Nevertheless, calcification depths derived from Mg/Ca-based temperatures yield reasonable habitat depths for *N. dutertrei* crust values compared to observations of *N. dutertrei* in stratified tows [e.g., *Bouvier-Soumagnac and Duplessy*, 1985; *Sautter and Thunell*, 1991; *Ravelo and Fairbanks*, 1992; *Wejnert et al*., 2013], potentially indicating similar Mg partitioning into the lamellar and crust calcite for this species. For *G. scitula* and *P. obliquiloculata*, this is not clear when considering Mg/Ca only.

4.2. Constraints on Crust and Cortex Formation From Observed Wall Thickness

Foraminiferal chamber walls generally increase in thickness by continued addition of calcite on all chambers exposed in the last whorl each time a new chamber forms. Foraminiferal chamber construction starts by formation of a thin organic layer (primary organic sheet (POS)) [*Banner et al*., 1973; *Hemleben et al*., 1977; *Hansen*, 1999], followed by deposition of calcite on both sides of the POS of both the newly formed chamber and on the outer surface of all preceding chambers of the last whorl. This successively enveloping of existing chambers results in the lamellar microstructure of test walls also seen in the chambers of the last whorl of all three species studied here. Increasing wall thickness toward the older chambers is clearest and statistically most significant in *N. dutertrei* and accompanied by a thickening of added crust calcite. This suggests that terminal crust formation is an ongoing process with most calcite added to the "oldest" chambers exposed in the final whorl. This is in line with the gradient in crustal Mg/Ca of successive chambers in *N. dutertrei*.

Although successive chambers of *P. obliquiloculata* show a trend in wall thickness, this trend is not significant, or at least not enough to statistically resolve (see Table 1 for statistical results). Cortex thickness in *P. obliquiloculata* is surprisingly uniform on all chambers of its final whorl (Figures 5b and 10, approximately 7.7 $\pm$0.3 μm), suggesting it is evenly added after the last chamber had formed. The simultaneous addition of cortex calcite over the entire shell is in line with its homogeneous Mg/Ca composition.

In line with its clear lamellar structure, *G. scitula* shows a statistically significant increase in wall thickness toward the older chambers in the final whorl (i.e., formed earlier). The crust calcite, although showing somewhat of a trend, is statistically uniform in thickness over the entire last whorl. As for *G. scitula*, this is in line with the Mg/Ca data for the crust calcite of the different successive chambers. Not only thickness of the crust and/or cortex provides information on its formation, also differences in appearance and surface structure may reflect processes involved.

4.3. Constraints From Morphology

Typical terminal features include crust and/or cortex formation (as here in *G. scitula*, *N. dutertrei* and *P. obliquiloculata*), gametogenic calcification, as well as the formation of a final diminutive (i.e., "kummerform")

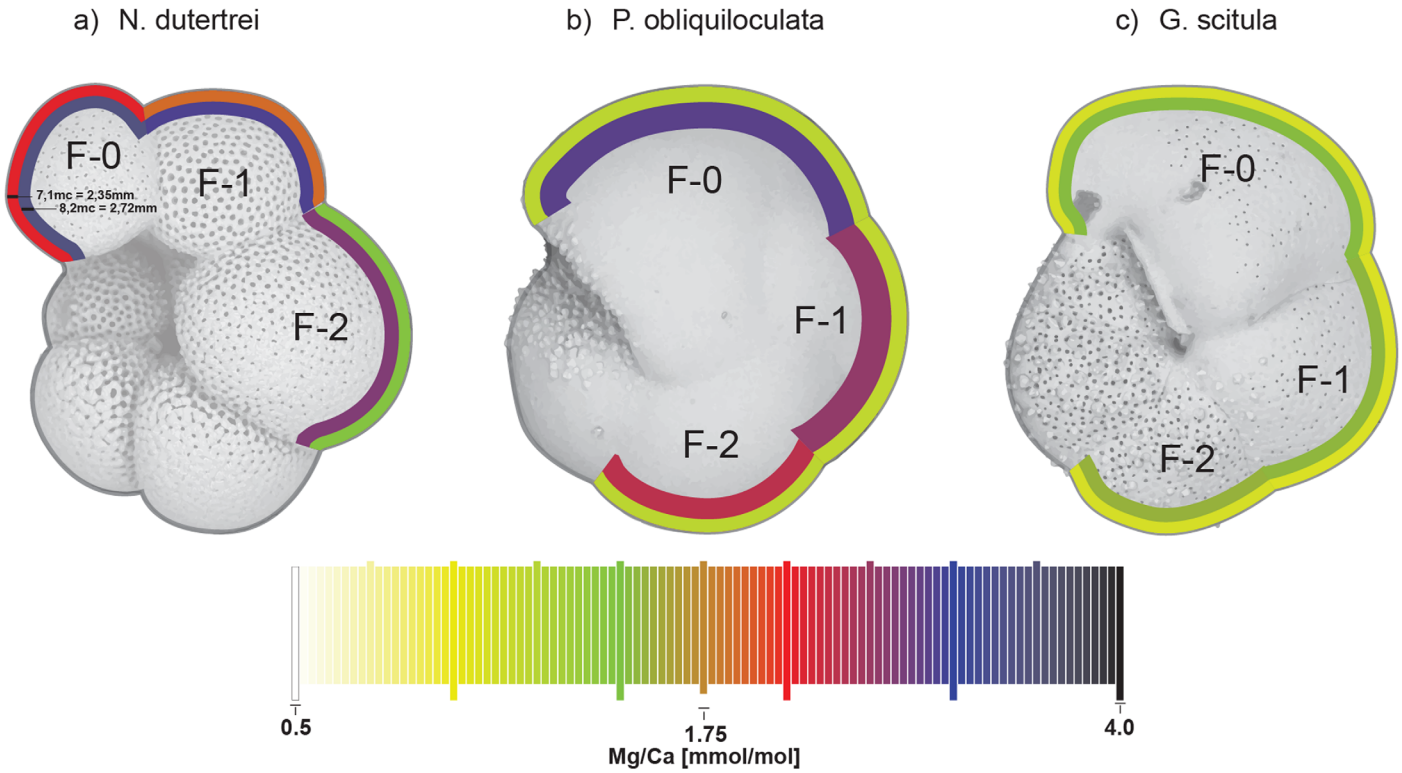

Figure 10. Schematic illustration for intra and interspecies crust and lamellar Mg/Ca values, as represented by color scale. Shell thickness, crust, and lamellar calcite are shown in scale for (a) *N. dutertrei*, (b) *P. obliquiloculata*, and (c) *G. scitula*.

chamber (or two of such chambers as observed here for *N. dutertrei*: Figures 10 and 11a) and/or a chamber of diagnostic shape (e.g., bulla, sphere, sack, and ampulla). The addition of a terminal cortex drastically changes the appearance of adult specimens of *P. obliquiloculata*. Whereas adult specimens have a thin, perforate shell with a hispid appearance, cortex formation thickens its walls, obliterates its pores and smoothens the outer shell completely (Figure 11b). Such drastic changes typically occur during late ontogeny of planktonic foraminifera, i.e., when adult shell growth stops and individuals enter the terminal stage of ontogeny in preparation for reproduction [*Brummer et al*., 1986, 1987; *Hemleben et al*., 1989]. The terminal stage is the last in a succession of five such ontogenetic stages that are recognized in planktonic foraminifera. All stages are marked by sudden transitions in shell morphology linked to changes in vital behavior, such as the changeover from an herbivorous to carnivorous diet in spinose species [*Brummer et al*., 1987]. Terminal stages mark the transition from growth to reproduction, including the deposition of an additional layer of gametogenic calcite immediately prior to gametogenesis in various spinose species [*Hemleben et al*., 1989]. *Burt and Scott* [1975] describe an ontogenetic change in *P. obliquiloculata* from a globigerine (juvenile) architecture during early ontogeny to a pulleniatine (adult) architecture later in ontogeny. Changes in shell morphological appearance thus define important transitions in life cycle.

Exemplary, *N. dutertrei* analyzed here have six chambers in its final whorl (Figure 11a), four of which typically result from adult growth (F-5 to F-2), i.e., are "normalform" chambers that increase exponentially in size. By contrast, the final two chambers are both diminutive ("kummerform"), i.e., are smaller than adult logarithmic shell growth predicts. The last two chambers probably result from terminal stage calcification that also produced the crust. Based on the gradual thinning of the crust after the F-1 chamber, this observation is in line with crust formation starting after adult F-2, i.e., together with the calcification of the first kummerform chamber. Since there are clear differences in crust Mg/Ca between the subsequent chambers (Figure 9), the earliest crustal layer on e.g., F-5 may well be deposited during calcification of the first kummerform chamber (F-1, with its aperture on F-5). Subsequently, the first crust on F-4 is deposited when the second kummerform chamber was produced (F-0) and also covered the preceding chambers, similar to lamellar calcification, and thus produced the gradients we observe in both Mg/Ca and wall thickness toward the

final chamber. Potentially crust formation may have continued much longer without addition of any additional new chamber, until gametogenesis concludes the life of the parent *N. dutertrei*.

Crust thickness in *N. dutertrei* appears to decrease toward the aperture and the sutures between chambers (Figures 4a and 4b), i.e., where the cytoplasm exits the shell. Hence, the microenvironment around the cytoplasma, which is influenced by active and passive element transport [*Bentov and Erez*, 2006; *De Nooijer et al*., 2014] may play a role in precipitation of crust and its distribution. Similarly, in various specimens of *P. obliquiloculata*, we found incisions into the cortex that diverge from the aperture (Figures 6a and 6b), which reflect the presence of pseudopodia during cortex formation, indicating that the specimen is alive and active while the cortex is precipitated, consistent with both its Mg/Ca value and its cortex thickness. As observed for *P. obliquiloculata* (Figure 12), the final whorl consists of five chambers, all of which are normal-form pulleniatine (i.e., adult-terminal streptospiral coiling); both specimens in Figure 11 are terminal stages given their cortex (early stage in Figure 11a, fully developed in Figure 11b). Apparently a cortex also differs from a crust in being precipitated equally over the entire outer shell instead of being concentrated on the earlier chambers and away from the aperture and sutures. Also, the cortex appears rather smooth over the entire shell in *P. obliquiloculata* (as in the spinose taxon *Sphaeroidinella dehiscens*) while the crust of *N. dutertrei* and *G. scitula* becomes increasingly more coarse crystalline toward the earliest chamber in the final whorl, suggesting that crusts on the "oldest" chamber form over a longer time span.

Pore diameters in *P. obliquiloculata* are drastically reduced by the formation of a cortex, changing their wide circular profile to narrow radiating fissures [*Burt et al*., 1971] (Figure 6b). Decreased porosity typically results from crust formation as well, as observed for both *G. scitula* and, to a lesser degree, *N. dutertrei*. Although the actual function of pores yet remains to be clarified, pores are characteristically abundant in living adult stages [*Be*, 1976], suggesting that a terminal reduction in porosity marks a changeover to a lower metabolic level that may have changed Mg/Ca partitioning during crust and cortex formation. Such a lower metabolic level may be caused by lower temperatures at greater depth. *Hemleben et al*. [1985] observed that crusts started form when freshly collected specimens of *G. truncatulinoides* were exposed to culture temperatures below 14–8°C.

For *G. scitula* as in Figure 11, we observed just over four chambers in its final whorl, which all seem normal-form adult-terminal. Being of similar thickness over the entire shell, crust formation would have started together with, or after the calcification of F-0 and may have continued/extended to other chambers later, potentially in wait for reproduction. This suggests that the crust or cortex might be somehow involved in protection, as calcite shells are generally thought to have originated as protective armors against predation that evolved during the Cambrian radiation [*Bengston*, 1994]. While no larger organisms are known that prey specifically on planktonic foraminifera, calcified shells do protect against viral or bacterial infections. Similarly, reduced pore diameters would help to safeguard the organism. Analogous to coccolithophorids this potentially might play a major role in governing mortality in populations of planktonic foraminifera. *Emiliani* [1993] named viral infections as one of the possible causes for foraminiferal extinctions.

In four specimens of *N. dutertrei*, we observed patches of crust inside the chamber wall (Figure 12). The fact that crust calcite also forms on the inside of the shell and seems to start precipitating around the pores makes a biological control likely. Albeit resulting in much thinner and patchier coverage, crust formation on the shell inside is in line with an internalized mode of crust and cortex formation that is consistent with the bilamellar biomineralization of planktonic foraminifera. Investigating the internal variability in chemistry within foraminiferal shell walls, *Eggins et al*. [2003] showed that the internal layering is symmetrical with respect to the POS. The layers formed towards the outside from the POS are, however, much thicker than the layers on the inside. Apparently this pattern is not restricted to the lamellar calcification only, but continues also during crust formation.

4.4. Interspecific Differences in Cortex and Crust Formation

4.4.1. *N. dutertrei*

The Mg/Ca data from crust and lamellar calcite, the decreasing crust thickness toward the final chamber and the overall appearance with larger crystals being deposited toward the aperture, suggest that crust formation in *N. dutertrei* proceeds sequentially. This would result in a gradual formation of the crust, starting before the last "kummerform" chambers are formed (Figure 11a). This hypothesis explains the thicker crust on earlier chambers, as these chambers are the exposed longest to accretion of crust calcite. Continued

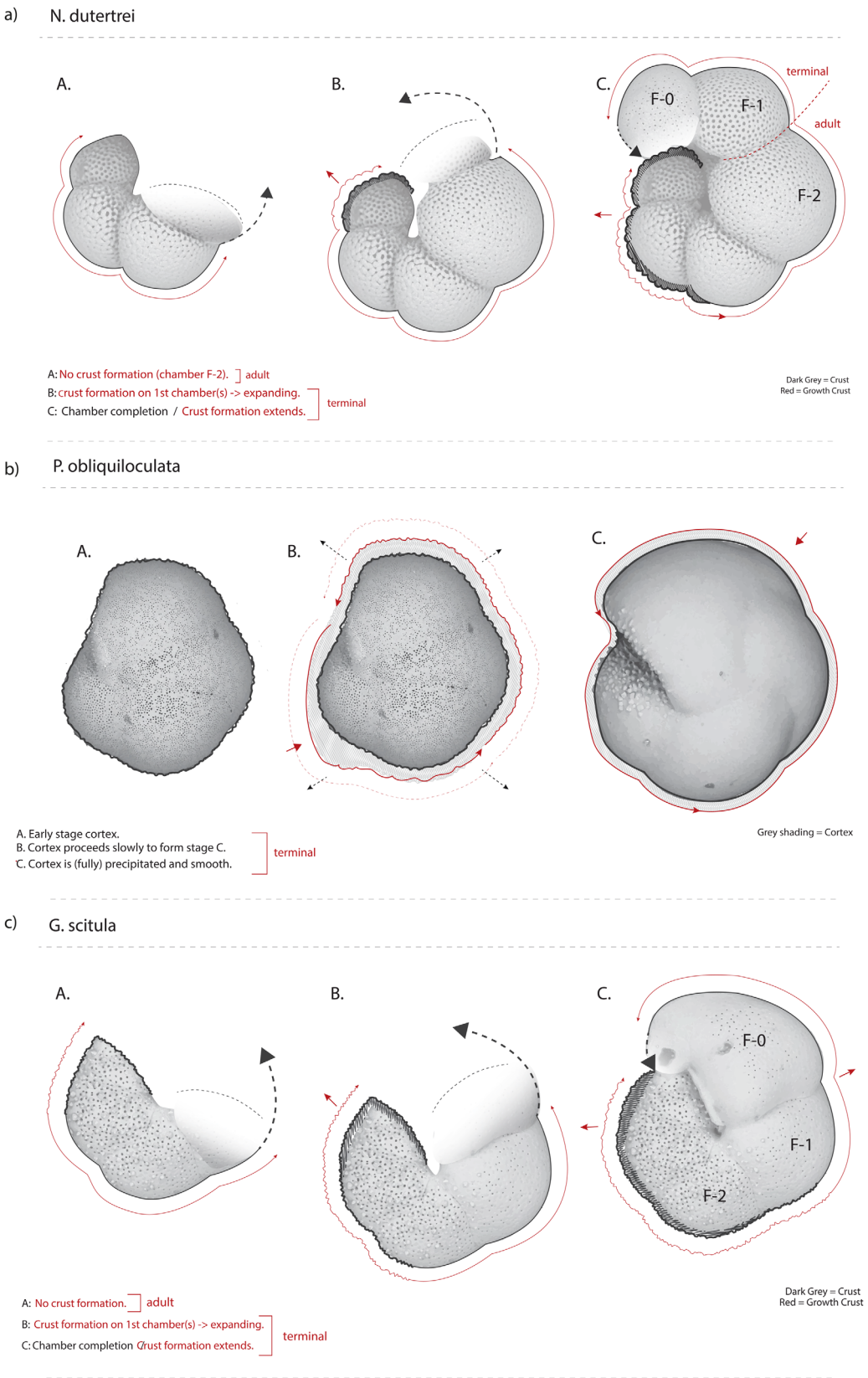

Figure 11. Schematic illustration of formation processes of crust in *N. dutertrei* (a), cortex in *P. obliquiloculata* (b), and crust in *G. scitula* (c). In *N. dutertrei*, crust starts to form in the terminal stage with the onset of chamber F-1 calcification. Crust formation in *G. scitula* takes place during or after the formation of the final chamber (F-0).

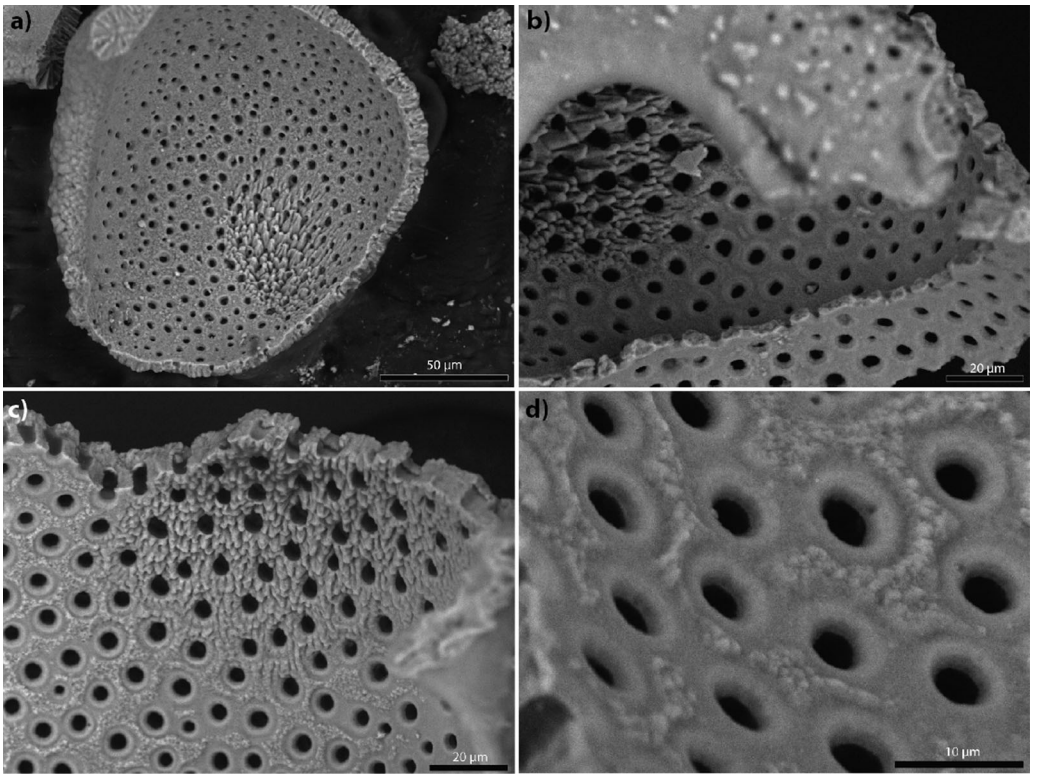

Figure 12. SEM images of *N. dutertrei*, exemplifying patchy crust-like features on the inner surface of the chamber wall as observed in four different specimens. Note that these crust-like features clearly are elevated above the surrounding shell surface (particularly Figures 12c and 12d), whereas dissolution features would result in depressions of the shell surface.

sequential addition of crust calcite also explains the observed gradients in crust Mg/Ca as these layers not necessarily formed at the same time. Differences in either temperature or related to vital effects therefore would cause offsets between the crust calcite added to the different chambers. The observed difference in crust Mg/Ca could hence potentially be related to the migration pattern of this foraminifera during the last phases of its life cycle.

4.4.2. *P. obliquiloculata*

In contrast to *N. dutertrei* and *G. scitula*, *P. obliquiloculata* shows no size-related trend in cortex Mg/Ca or in cortex thickness (see Table 1 for statistical results). It is therefore likely that the cortex formed under similar conditions and within a similar time frame. Since the last chamber is also covered by the cortex, it must have formed after the last chamber was added, via biologically controlled precipitation (Figure 11b) judging from the cytoplasmatic striae on its outer surface near the aperture (Figures 6a and 6b). The low Mg/Ca ratios of the cortex could reflect both lower temperatures during its formation and/or enhanced partitioning against Mg during the terminal stage. A slower metabolic rate during the late stages of a foraminiferal life cycle [*Hemleben et al*., 1989] might reduce active Ca-ion transport into the cell, which would also lower leakage of ions such as Mg [*Nehrke et al*., 2013]. This would thereby result in slow growth of the cortex and a low Mg/Ca. In some cases we observe small variations in Mg/Ca within the cortex (Figure 13), which may thus indicate a modest depth migration of the species during the formation of the cortex or slight changes in metabolic activity. Either way such internal variability suggests that cortex formation is a prolonged process rather than an instantaneous event, which is in line with the observed imprints of a (locally dense) pseudopodial network.

P. obliquiloculata has been suggested to have an annual production cycle [e.g., *Jonkers et al*., 2015; *Salmon et al*., 2015], with a terminal cortex possibly forming over months and reflecting a deep inactive (diapausing) stage between reproductive peaks. For example, *Hemleben et al*. [1985] showed crust formation for *G. truncatulinoides* in a culture study and although no exact timing was indicated this involved a few weeks at most. The limited time involved with crust formation implies that alternatively a terminal crust or cortex

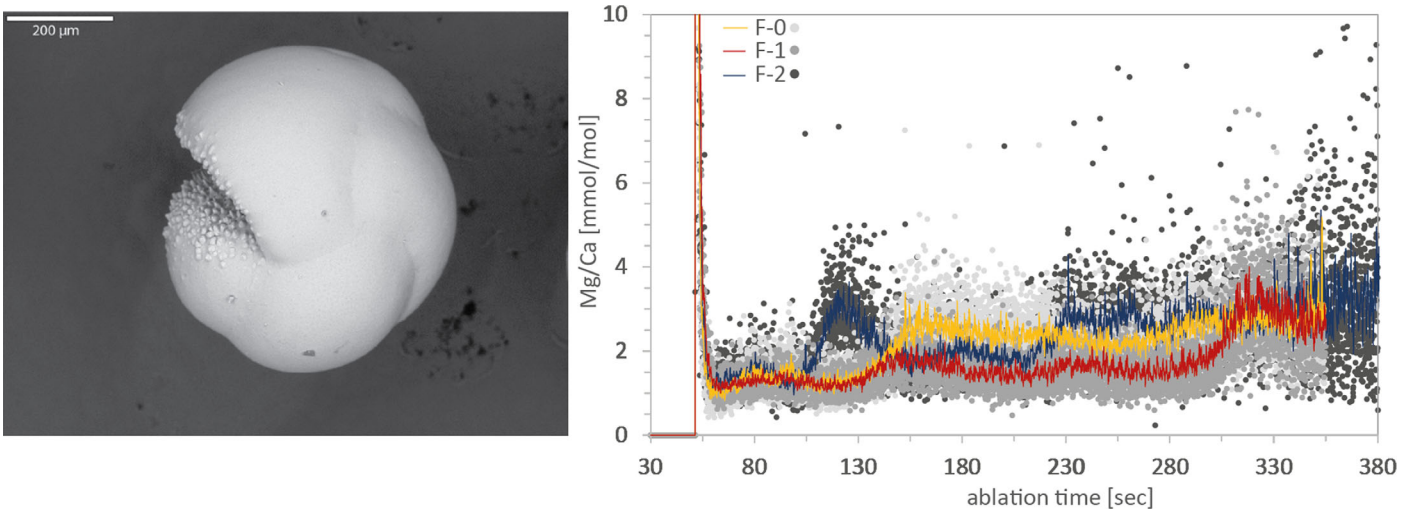

Figure 13. Scanning electron microscope (SEM) images of *P. obliquiloculata*. On the right the LA-ICP-MS raw (greyish points) and nine point running average (colored dots) Mg/Ca profiles of several chambers from the same specimens. Note the Mg/Ca variability within the low Mg/Ca part of the cortex.

could have formed relatively fast (days to weeks) at the beginning of a resting stage. Resting stages have been reported for phytoplankton (i.e., dinoflagellates) and zooplankton taxa such as rotifers, tintinids, cnidarians, and copepods [*Paranjape*, 1980; *Dale*, 1983; *Pouriot and Snell*, 1983; *Boero et al*., 1992; *Marcus*, 1996]. Entering a dormant stage has been associated with countering adverse/unfavorable environmental conditions [e.g., *Marcus*, 1980, 1984; *Elgmork et al*., 1990], may occur seasonally (hibernation), and protect from predation [e.g., *Hairston and Olds*, 1984]. Here we hypothesize that some planktonic foraminiferal species may also have a dormant stage, which in the case of *P. obliquiloculata* is reflected by the cortex layer.

4.4.3. *G. scitula*

Crust thickness decreases slightly toward the younger chambers in *G. scitula* (Jonckheere-Terpstra test, $p = 0.04$), similar to but less so than in *N. dutertrei*. In line with *P. obliquiloculata*, the lack of differences in Mg/Ca and minor change in crust thickness suggest a more or less synchronous crust deposition over the entre shell. Still, in contrast to *P. obliquiloculata* we recognize pustule-like structures near the aperture (Figure 6d). Crust formation in *G. scitula* therefore seems to be related to that of both *N. dutertrei* and *P. obliquiloculata* (Figure 11c). Given the deep habitat of *G. scitula*, changes in calcification depth during crust formation would only cause little temperature-induced variability in crust Mg/Ca. Alternatively depth migration by *G. scitula* may have been limited during its late ontogenetic stage. In fact the only differences observed in Mg/Ca of *G. scitula* are between crust and lamellar calcite in all four chambers. Consequently, the only depth migration that may have occurred, should have occurred right between the end of lamellar calcification and the start of crust formation in order to explain the contrast in crust and lamellar Mg/Ca. In our opinion it is highly unlikely that there would have been a kind of pausing during which no shell growth nor encrustation occurs, while the specimen settles down a few hundred meters, and subsequently resuming with encrustation.

4.5. Implications: Effects of Crust on Paleoreconstructions

Patterns in crust and cortex thickness as well as composition suggest that these test features may formed over a prolonged time period and, at least for *P. obliquiloculata*, may reflect a deep resting stage. Resting stages might be a common feature in the life cycle of planktonic foraminifera in species that only show a single, sharp peak in abundance during the year. Such species include *P. obliquiloculata*, *G. scitula*, *G. truncatulinoides*, *G. hirsuta* and *G. tumida* [e.g., *Deuser*, 1986; *Mohtadi et al*., 2009; *Salmon et al*., 2015] which are typically encrusted and only bloom in winter when surface temperatures are relatively low and the water column is deeply mixed. In between two annual peaks, a very small population persists judging from observed trace shell fluxes [*Wilke et al*., 2009], and it is such a persistent population that will reproductively generate peak fluxes the next year. In high-latitude settings, the trace fluxes in winter regard survivors from the previous summer maximum, given their stable isotope signature [*Jonkers et al*., 2010]. Virtually no living planktonic foraminifera are found below 1000 m [*Vincent and Berger*, 1981] and there are no confirmed

reports of living (or resting) planktonic foraminifera on the sea floor [*Kucera*, 2007]. Although some benthic species exhibit a complex life cycle including an array of reproductive strategies [e.g., *Alve and Goldstein*, 2003; *Goldstein*, 2003], planktonic species are only known to reproduce sexually [see *Hemleben et al*., 1989]. To increase reproduction chances, gamete release by different specimens from the same species may be synchronized in space and time. *Wilke et al*. [2009] used plankton net and sediment traps to show that *P. obliquiloculata* abounds in the surface mixed layer during winter, while absent or in trace abundances in or below the surface mixed layer during other seasons. For *G. truncatulinoides*, *Loncaric et al*. [2006] found a similar winter maximum throughout the upper 150 m, contrasting with low summer concentrations below the surface mixed layer. Whether sharp peaks in abundance during winter represent an annual reproduction cycle or a short period of rapid overturning in multiple generations yet remains to be determined [*Loncaric et al*., 2006]. Still, the specimens releasing gametes ultimately growing into the next generation have to be present throughout the year. A resting stage of *P. obliquiloculata* would mechanistically link life cycle and a single annual reproductive pulse.

The difference in composition of crust and lamellar calcite also potentially affects the application of Mg/Ca as temperature proxy, if applied on whole single shells. In specimens of *N. dutertrei*, crust Mg/Ca can be 10–20% lower than that of the lamellar calcite. In *P. obliquiloculata* and *G. scitula*, Mg/Ca of the crust is approximately 13–18% and 3–11% lower, respectively. Due to variability in crust thickness, the contribution of the crust to the total specimen's Mg/Ca is also variable between species and to a lesser extent, within species. In *N. dutertrei* we find a gradual decrease of crust Mg/Ca contribution onto the average Mg/Ca composition, while the crust contributes on average 46% to its total wall thickness. In *P. obliquiloculata* we find that the average Mg/Ca composition of the F-2 chamber is slightly less affected (13.1%) than the F-1 and F-0 chamber (17.2 and 17.8%, respectively), while its cortex makes up an average 32% of the total wall thickness. Interestingly, the average Mg/Ca composition of the F-2 chamber in *G. scitula* is most affected by its crust (11.4% lower than lamellar calcite) and lowest for F-3 (2.9%). On average, the crust in *G. scitula* contributes 47% to the total wall thickness. Mg/Ca-temperatures can be biased by varying thicknesses of low Mg/Ca crust and/or cortex contributions to the whole shell Mg/Ca. Applying a simple mass balance, with changing crust contributions we can assess changes to the total shell composition and its implications on Mg/Ca temperature reconstructions.

Previous studies have shown that shell thickness can vary on glacial/interglacial time scales and between ocean basins [e.g., *Barker and Elderfield*, 2002; *De Moel et al*., 2009]. Assuming a crust contribution of 50% to the total wall thickness in *N. dutertrei*, average crustal Mg/Ca (Figure 8b) temperatures are estimated to be 22.2°C. If the crust makes up 75% of the wall, Mg/Ca-based temperature would decrease by about 3.5°C; if the crust however only contributes 25%, Mg/Ca-based temperatures would increase by 1°C. In *P. obliquiloculata*, a cortex contribution of just 25% to the total wall thickness affects Mg/Ca-based temperatures more so than in *N. dutertrei*, as a 25% cortex contribution would result in a 2.1°C higher temperature estimate compared to a 50% cortex contribution (20.2°C). A 75% cortex contribution has an equally strong effect, decreasing Mg/Ca temperature by approximately 2.6°C. In *G. scitula*, low Mg/Ca crust affects average wall Mg/Ca less than in *P. obliquiloculata*. Temperature estimates decrease by about 1.3°C for every 25% of crust calcite added. Hence, varying contributions of crust and/or cortex calcite may introduce significant scatter on whole wall Mg/Ca-based temperature reconstructions of single specimens.

5. Conclusions

We analyzed crust/cortex Mg/Ca with LA-ICP-MS and measured crust/cortex as well as total wall thicknesses on three species of planktonic foraminifera (*N. dutertrei*, *P. obliquiloculata* and *G. scitula*) from sediment trap samples. All species analyzed have a lower crust/cortex Mg/Ca than their lamellar calcite. Additionally, crust/cortex Mg/Ca differs between species. Only *N. dutertrei* shows increasing crust Mg/Ca values toward its last chambers. Using crust/cortex Mg/Ca and wall thicknesses, we constructed a conceptual model for all three species to reconstruct growth pattern and crust/cortex formation. The results suggest different processes for crust and cortex formation. *N. dutertrei* and to a lesser degree potentially also *G. scitula*, seem to precipitate crust gradually while still adding chambers, leading to a thinning of the crust towards the younger chambers. The trend in crust Mg/Ca, found in *N. dutertrei* is likely caused by migration during the

later stages of its life. For *P. obliquiloculata*, slow precipitation of cortex after the last chamber has been formed is more likely.

Acknowledgments
Data are available and can be requested from the corresponding author (juliane.steinhardt@nioz.nl). We acknowledge funding from the European Commission 7th Framework Marie Curie People program FP7/2007–2013 through funding of the Initial Training Network "GATEWAYS" (www.gatewaysitn.eu) under the grant 238512. Furthermore we acknowledge funding from the LOCO- and INATEX-programs. Analyses and visualizations of satellite SST used in this paper were produced with the Giovanni online data system, developed and maintained by the NASA GES DISC. We thank the chief scientist Herman Ridderinkhof and the crew of the RRV Charles Darwin, RRV Discovery, FS Meteor, RV Pelagia, and RV Algoa. Great thanks to Wim Boer for providing technical support with the trace element analysis at NIOZ and Helen de Waard and Michiel Kienhuis at the University Utrecht. Furthermore, we thank the EMAP Lab at University of Utrecht as well as Jan Berend Stuut for the usage of the Hitachi High-Tech TM3000 tabletop microscope.

References

Allison, N., and W. E. N. Austin (2003), The potential of ion microprobe analysis in detecting geochemical variations across individual foraminifera tests, *Geochem. Geophys. Geosyst.*, *4*(2), 8403, doi:10.1029/2002GC000430.

Alve, E., and S. T. Goldstein (2003), Propagule transport as a key method of dispersal in benthic foraminifera (Protista), *Limnol. Oceanogr.*, *48*(6), 2163–2170.

Anand, P., H. Elderfield, and M. Conte (2003), Calibration of Mg/Ca thermometry in planktonic foraminifera from a sediment trap time series, *Paleoceanography*, *18*(2), 1050, doi:10.1029/2002PA000846.

Banner, F., R. Sheehan, and E. Williams (1973), The organic skeletons of rotaline foraminifera: A review, *J. Foraminiferal Res.*, *3*(1), 30–42.

Barker, S., and Elderfield, H. (2002), Foraminiferal calcification response to glacial-interglacial changes in atmospheric CO_2, *Science*, *297*(5582), 833–836.

Bé, A. W. (1969), Planktonic foraminifera, *Antarct. Map Folio Ser. Am. Geogr. Soc.*, *11*, 9–12.

Bé, A. W. H. (1960), Ecology of recent planktonic foraminifera-Part 2: Bathymetric and seasonal distributions in the Sargasso Sea off Nermuda, *Micropaleontology*, *6*(4), 373–392.

Bé, A. W. H. (1980), Gametogenic calcification in a spinose planktonic foraminifer, *Globigerinoides sacculifer* (Brady), *Mar. Micropaleontol.*, *5*, 283–310, doi:10.1016/0377–8398(80)90014-6.

Bé, A. W., and W. H. Hutson (1977), Ecology of planktonic foraminifera and biogeographic patterns of life and fossil assemblages in the Indian Ocean, *Micropaleontology*, *23*(4), 369–414.

Bemis, B. E., H. J. Spero, D. W. Lea, and J. Bijma (2000), Temperature influence on the carbon isotopic composition of *Globigerina bulloides* and *Orbulina universa* (planktonic foraminifera), *Mar. Micropaleontol.*, *38*(3–4), 213–228, doi:10.1016/S0377-8398(00)00006-2.

Bentov, S., and J. Erez (2006), Impact of biomineralization processes on the Mg content of foraminiferal shells: A biological perspective, *Geochem. Geophys. Geosyst.*, *7*, Q01P08, doi:10.1029/2005GC001015.

Boero, F., J. Bouillon, and S. Piraino (1992), On the origins and evolution of hydromedusan life cycles (Cnidaria, Hydrozoa), *Sex Origin Evol.*, *6*, 59–68.

Bouvier-Soumagnac, Y., and J.-C. Duplessy (1985), Carbon and oxygen isotopic composition of planktonic foraminifera from laboratory culture, plankton tows and recent sediment; implications for the reconstruction of paleoclimatic conditions and of the global carbon cycle, *J. Foraminiferal Res.*, *15*(4), 302–320.

Boyle, E. A. (1981), Cadmium, zinc, copper, and barium in foraminifera tests, *Earth Planet. Sci. Lett.*, *53*(1), 11–35, doi:10.1016/0012-821X(81)90022-4.

Bengston, S. (1994), The advent of animal skeletons, in *Early Life on Earth, Nobel Symposium 84*, edited by S. Bengtson, pp. 412–425, Columbia Univ. Press, N. Y.

Brummer, G.-J. A., C. Hemleben, and M. Spindler (1987), Ontogeny of extant spinose planktonic foraminifera (Globigerinidae): A concept exemplified by *Globigerinoides sacculifer* (Brady) and *G. ruber* (d'Orbigny), *Mar. Micropaleontol.*, *12*, 357–381, doi:10.1016/0377-8398(87)90028-4.

Burt, B. J., and G. H. Scott (1975), Spinosity and coiling geometry in Pulleniatina (Foraminiferida), *J. Foraminiferal Res.*, *5*(3), 166–175, doi:10.2113/gsjfr.5.3.166.

Cléroux, C., E. Cortijo, J. Duplessy, and R. Zahn (2007), Deep-dwelling foraminifera as thermocline temperature recorders, *Geochem. Geophys. Geosyst.*, *8*, Q04N11, doi:10.1029/2006GC001474.

Cléroux, C., E. Cortijo, P. Anand, L. Labeyrie, F. Bassinot, N. Caillon, and J.-C. Duplessy (2008), Mg/Ca and Sr/Ca ratios in planktonic foraminifera: Proxies for upper water column temperature reconstruction, *Paleoceanography*, *23*, PA3214, doi:10.1029/2007pa001505.

Dale, B. (1983), Dinoflagellate resting cysts: "Benthic plankton," in *Survival Strategies Of the Algae*, pp. 69–136, Cambridge University Press, Cambridge, Mass.

De Moel, H., G. M. Ganssen, F. J. C. Peeters, S. J. A. Jung, D. Kroon, G. J. A. Brummer, and R. E. Zeebe (2009), Planktic foraminiferal shell thinning in the Arabian Sea due to anthropogenic ocean acidification, *Biogeosciences*, *6*(9), 1917–1925.

De Nooijer, L. J., H. J. Spero, J. Erez, J. Bijma, and G. J. Reichart (2014), Biomineralization in perforate foraminifera, *Earth Sci. Rev.*, *135*, 48–58, doi:10.1016/j.earscirev.2014.03.013.

Dekens, P. S., D. W. Lea, D. K. Pak, and H. J. Spero (2002), Core top calibration of Mg/Ca in tropical foraminifera: Refining paleotemperature estimation, *Geochem. Geophys. Geosyst.*, *3*(4), 1022, doi:10.1029/2001GC000200.

Deuser, W. (1986), Seasonal and interannual variations in deep-water particle fluxes in the Sargasso Sea and their relation to surface hydrography, *Deep Sea Res. Oceanogr. Res. Pap.*, *33*, 225–246.

Duckworth, D. L. (1977), Magnesium concentration in the tests of the planktonic foraminifer *Globorotalia truncatulinoides*, *J. Foraminiferal Research*, *7*, 304–312, doi:10.2113/gsjfr.7.4.304.

Eggins, S., P. De Deckker, and J. Marshall (2003), Mg/Ca variation in planktonic foraminifera tests: Implications for reconstructing palaeo-seawater temperature and habitat migration, *Earth Planet. Sci. Lett.*, *212*, 291–306.

Eggins, S. M., A. Sadekov, and P. De Deckker (2004), Modulation and daily banding of Mg/Ca in *Orbulina universa* tests by symbiont photosynthesis and respiration: A complication for seawater thermometry?, *Earth Planet. Sci. Lett.*, *225*(3–4), 411–419, doi:10.1016/j.epsl.2004.06.019.

Elgmork, K., G. Halvorsen, J. Eie, and A. Langeland (1990), Coexistence with similar life cycles in two species of freshwater copepods (Crustacea), *Hydrobiologia*, *208*(3), 187–199.

Emiliani, C. (1993), Extinction and viruses, *Biosystems*, *31*(2–3), 155–159, doi:10.1016/0303-2647(93)90044-D.

Epstein, S., R. Buchsbaum, H. Lowenstam, and H. C. Urey (1951), Carbonate-water isotopic temperature scale, *Geol. Soc. Am. Bull.*, *62*(4), 417–426, doi:10.1130/0016-7606(1951)62[417:CITS]2.0.CO;2.

Erez, J. (2003), The source of ions for biomineralization in foraminifera and their implications for paleoceanographic proxies, *Rev. Mineral. Geochem.*, *54*, 115–149.

Erez, J., and S. Honjo (1981), Comparison of isotopic composition of planktonic foraminifera in plankton tows, sediment traps and sediments, *Palaeogeogr. Palaeoclimatol. Palaeoecol.*, *33*, 129–156, doi:10.1016/0031-0182(81)90035-3.

Evans, D., and W. Müller (2013), LA-ICPMS elemental imaging of complex discontinuous carbonates: An example using large benthic foraminifera, *J. Anal. At. Spectrom.*, *28*(7), 1039–1044, doi:10.1039/C3JA50053E.

Fairbanks, R. G., P. H. Wiebe, and A. W. Bé (1980), Vertical distribution and isotopic composition of living planktonic foraminifera in the western North Atlantic, *Science*, *207*, 61–63.
Fairbanks, R. G., M. Sverdlove, R. Free, P. H. Wiebe, and A. W. Bé (1982), Vertical distribution and isotopic fractionation of living planktonic foraminifera from the Panama Basin, *Nature*, *298*, 841–844.
Fallet, U., W. Boer, C. van Assen, M. Greaves, and G.-J. A. Brummer (2009), A novel application of wet oxidation to retrieve carbonates from large organic-rich samples for ocean-climate research, *Geochem. Geophys. Geosyst.*, *10*, Q08004, doi:10.1029/2009gc002573.
Fallet, U., G.-J. Brummer, J. Zinke, S. Vogels, and H. Ridderinkhof (2010), Contrasting seasonal fluxes of planktonic foraminifera and impacts on paleothermometry in the Mozambique Channel upstream of the Agulhas Current, *Paleoceanography*, *25*, PA4223, doi:10.1029/2010pa001942.
Fallet, U., J. E. Ullgren, I. S. Castañeda, H. M. van Aken, S. Schouten, H. Ridderinkhof, and G.-J. A. Brummer (2011), Contrasting variability in foraminiferal and organic paleotemperature proxies in sedimenting particles of the Mozambique Channel (SW Indian Ocean), *Geochim. Cosmochim. Acta*, *75*(20), 5834–5848.
Fehrenbacher, J., and P. A. Martin (2010), Mg/Ca variability of the planktonic foraminifera *G. ruber s.s.* and *N. dutertrei* from shallow and deep cores determined by electron microprobe image mapping, *IOP Conf. Ser. Earth Environ. Sci.*, *9*(1), 012018, doi:10.1088/1755-1315/9/1/012018.
Fehrenbacher, J. S., and P. A. Martin (2014), Exploring the dissolution effect on the intrashell Mg/Ca variability of the planktic foraminifer *Globigerinoides ruber*, *Paleoceanography*, *29*, 854–868, doi:10.1002/2013PA002571.
Field, D. B. (2004), Variability in vertical distributions of planktonic foraminifera in the California Current: Relationships to vertical ocean structure, *Paleoceanography*, *19*, PA2014, doi:10.1029/2003PA000970.
Fischer, G. and G. Wefer (Eds.) (1999). *Use of Proxies in Paleoceanography*, 735 pp., Springer, Berlin.
Goldstein, S. T. (2003), Foraminifera: A biological overview, in *Modern Foraminifera*, edited by B. K. Sen Gupta, pp. 37–55, Springer, Netherlands.
Hairston, N. G., Jr., and E. J. Olds (1984), Population differences in the timing of diapause: Adaptation in a spatially heterogeneous environment, *Oecologia*, *61*(1), 42–48.
Hathorne, E., O. Alard, R. James, and N. Rogers (2003), Determination of intratest variability of trace elements in foraminifera by laser ablation inductively coupled plasma-mass spectrometry, *Geochem. Geophys. Geosyst.*, *4*(12), 8408, doi:10.1029/2003GC000539.
Hemleben, C., and M. Spindler (1983), Recent advances in research on living planktonic foraminifera, *Utrecht Micropaleontol. Bull.*, *30*, 141–170.
Hemleben, C., A. W. H. Be, O. R. Anderson, and S. Tuntivate (1977), Test morphology, organic layers and chamber formation of the planktonic foraminifer *Globorotalia menardii* (d'Orbigny), *J. Foraminiferal Res.*, *7*(1), 1–25, doi:10.2113/gsjfr.7.1.1.
Hemleben, C., M. Spindler, I. Breitinger, and W. G. Deuser (1985), Field and laboratory studies on the ontogeny and ecology of some globorotaliid species from the Sargasso Sea off Bermuda, *J. Foraminiferal Res.*, *15*(4), 254–272, doi:10.2113/gsjfr.15.4.254.
Hemleben, C., M. Spindler, and O. Anderson (1989), *Modern Planktonic Foraminifera*, 363 pp., Springer, Berlin.
Huang, K., C. You, H. Lin, and Y. Shieh (2008), In situ calibration of Mg/Ca ratio in planktonic foraminiferal shell using time series sediment trap: A case study of intense dissolution artifact in the South China Sea, *Geochem. Geophys. Geosyst.*, *9*, Q04016, doi:10.1029/2007GC001660.
Itou, M., T. Ono, T. Oba, and S. Noriki (2001), Isotopic composition and morphology of living *Globorotalia scitula*: A new proxy of subintermediate ocean carbonate chemistry?, *Mar. Micropaleontol.*, *42*, 189–210, doi:10.1016/S0377-8398(01)00015-9.
Jonkers, L., G.-J. A. Brummer, F. J. C. Peeters, H. M. van Aken, and M. F. De Jong (2010), Seasonal stratification, shell flux, and oxygen isotope dynamics of left-coiling *N. pachyderma* and *T. quinqueloba* in the western subpolar North Atlantic, *Paleoceanography*, *25*, PA2204, doi:10.1029/2009PA001849.
Jonkers, L., L. de Nooijer, G. Reichart, R. Zahn, and G. Brummer (2012), Encrustation and trace element composition of *Neogloboquadrina dutertrei* assessed from single chamber analyses, implications for paleotemperature estimates, *Biogeosciences*, *9*, 4851–4860.
Jonkers, L., C. E. Reynolds, J. Richey, and I. R. Hall (2015), Lunar periodicity in the shell flux of some planktonic foraminifera in the Gulf of Mexico, *Biogeosc.*, *12*, 3061–3070, doi:10.5194/bg-12-3061-2015.
Katz, M. E., B. S. Cramer, A. Franzese, B. Hönisch, K. G. Miller, Y. Rosenthal, and J. D. Wright (2010), Traditional and emerging geochemical proxies in foraminifera, *J. Foraminiferal Res.*, *40*(2), 165–192, doi:10.2113/gsjfr.40.2.165.
Kucera, M. (2007), Chapter six planktonic foraminifera as tracers of past oceanic environments, *Dev. Mar. Geol.*, *1*, 213–262.
Kunioka, D., K. Shirai, N. Takahata, Y. Sano, T. Toyofuku, and Y. Ujiie (2006), Microdistribution of Mg/Ca, Sr/Ca, and Ba/Ca ratios in *Pulleniatina obliquiloculata* test by using a NanoSIMS: Implication for the vital effect mechanism, *Geochem. Geophys. Geosyst.*, *7*, Q12P20, doi:10.1029/2006GC001280.
Kuroyanagi, A., and H. Kawahata (2004), Vertical distribution of living planktonic foraminifera in the seas around Japan, *Mar. Micropaleontol.*, *53*, 173–196.
Loncaric, N., F. J. C. Peeters, D. Kroon, and G. J. A. Brummer (2006), Oxygen isotope ecology of recent planktic foraminifera at the central Walvis Ridge (SE Atlantic), *Paleoceanography*, *21*, PA3009, doi:10.1029/2005PA001207.
Lunneborg, C. E. 2005. Jonckheere–Terpstra test, in *Encyclopedia of Statistics in Behavioral Science*, edited by B. S. Everitt and D. Howell, 2352 pp., John Wiley, N. Y.
Mann, H. B., and D. R. Whitney (1947), On a test of whether one of two random variables is stochastically larger than the other, *Ann. Math. Stat.*, *18*(1), 50–60.
Marcus, N. H. (1980), Photoperiodic control of diapause in the marine calanoid copepod *Labidocera aestiva*, *Biol. Bull.*, *159*(2), 311–318.
Marcus, N. H. (1984), Variation in the diapause response of *Labidocera aestiva* (Copepoda: Calanoida) from different latitudes and its importance in the evolutionary process, *Biol. Bull.*, *166*(1), 127–139.
Marcus, N. H. (1996), Ecological and evolutionary significance of resting eggs in marine copepods: Past, present, and future studies, *Hydrobiologia*, *320*(1–3), 141–152.
McCrea, J. M. (1950), On the isotopic chemistry of carbonates and a paleotemperature scale, *J. Chem. Phys.*, *18*(6), 849–857, doi:10.1063/1.1747785.
Mohtadi, M., S. Steinke, J. Groeneveld, H. G. Fink, T. Rixen, D. Hebbeln, B. Donner, and B. Herunadi (2009), Low-latitude control on seasonal and interannual changes in planktonic foraminiferal flux and shell geochemistry off south Java: A sediment trap study, *Paleoceanography*, *24*, PA1201, doi:10.1029/2008PA001636.
Mücke, S. K., and H. Oberhänsli (1999), The distribution of living planktic foraminifera in relation to southeast Atlantic oceanography, in *Use of Proxies in Paleoceanography*, edited by D. G. Fischer and P. D. G. Wefer, pp. 91–115, Springer, Berlin.
Nehrke, G., N. Keul, G. Langer, L. J. de Nooijer, J. Bijma, and A. Meibom (2013), A new model for biomineralization and trace-element signatures of Foraminifera tests, *Biogeosciences*, *10*(10), 6759–6767, doi:10.5194/bg-10-6759-2013.

Nooijer, L. J. de, T. Toyofuku, and H. Kitazato (2009), Foraminifera promote calcification by elevating their intracellular pH, *Proc. Natl. Acad. Sci. U. S. A.*, *106*(36), 15,374–15,378, doi:10.1073/pnas.0904306106.
Nürnberg, D., J. Bijma, and C. Hemleben (1996), Assessing the reliability of magnesium in foraminiferal calcite as a proxy for water mass temperatures, *Geochim. Cosmochim. Acta*, *60*(5), 803–814, doi:10.1016/0016-7037(95)00446-7.
Ortiz, J., A. Mix, W. Rugh, J. Watkins, and R. Collier (1996), Deep-dwelling planktonic foraminifera of the northeastern Pacific Ocean reveal environmental control of oxygen and carbon isotopic disequilibria, *Geochim. Cosmochim. Acta*, *60*, 4509–4523.
Paranjape, M. A. (1980), Occurrence and significance of resting cysts in a hyaline tintinnid, *Helicostomella subulata*(Ehre.) Jorgensen, *J. Exp. Mar. Biol. Ecol.*, *48*(1), 23–33.
Pena, L., E. Calvo, I. Cacho, S. Eggins, and C. Pelejero (2005), Identification and removal of Mn-Mg-rich contaminant phases on foraminiferal tests: Implications for Mg/Ca past temperature reconstructions, *Geochem. Geophys. Geosyst.*, *6*, Q09P02, doi:10.1029/2005GC000930.
Pflaumann, U., and Z. Jian (1999), Modern distribution patterns of planktonic foraminifera in the South China Sea and western Pacific: A new transfer technique to estimate regional sea-surface temperatures, *Mar. Geol.*, *156*, 41–83.
Pourriot, R., and T. W. Snell (1983), Resting eggs in rotifers, *Hydrobiologia*, *104*(1), 213–224.
Ramsey, P. H. (2000). Nonparametric statistical methods, *Technometrics*, *42*(2), 217–218, doi:10.1080/00401706.2000.10486020.
Ravelo, A., and R. Fairbanks (1992), Oxygen isotopic composition of multiple species of planktonic foraminifera: Recorders of the modern photic zone temperature gradient, *Paleoceanography*, *7*(6), 815–831, doi:10.1029/92PA02092.
Reichart, G.-J., F. Jorissen, P. Anschutz, and P. R. Mason (2003), Single foraminiferal test chemistry records the marine environment, *Geology*, *31*(4), 355–358.
Regenberg, M., S. Steph, D. Nürnberg, R. Tiedemann, and D. Garbe-Schönberg (2009), Calibrating Mg/Ca ratios of multiple planktonic foraminiferal species with δ^{18}O-calcification temperatures: Paleothermometry for the upper water column, *Earth Planet. Sci. Lett.*, *278*(3–4), 324–336, doi:10.1016/j.epsl.2008.12.019.
Reiss, Z. E. E. V. (1957), The Bilamellidea, nov. superfam., and remarks on Cretaceous Globorotaliids, *Cushman Found. Foram. Res*, *8*, 127–145.
Reiss, Z. (1959), The wall-structure of Cibicides, Planulina, Gyroidinoides, and Globorotalites, *Micropaleontology*, *5*(3), 355–357, doi:10.2307/1484428.
Reiss, Z. (1960), Structure of so-called Eponides and some other rotaliiform Foraminifera, State of Israel, Minist. of Dev., Israel, Geol. Surv. Bull. No. 29, pp. 1–28, pls. 1-3, tfs. 1-2.
Sadekov, A. Y., S. M. Eggins, and P. De Deckker (2005), Characterization of Mg/Ca distributions in planktonic foraminifera species by electron microprobe mapping, *Geochem. Geophys. Geosyst.*, *6*, Q12P06, doi:10.1029/2005GC000973.
Salmon, K. H., P. Anand, P. F. Sexton, and M. Conte (2015), Upper ocean mixing controls the seasonality of planktonic foraminifer fluxes and associated strength of the carbonate pump in the oligotrophic North Atlantic, *Biogeosciences*, *12*(1), 223–235, doi:10.5194/bg-12-223-2015.
Sautter, L. R., and R. C. Thunell (1991), Planktonic foraminiferal response to upwelling and seasonal hydrographic conditions; sediment trap results from San Pedro Basin, Southern California Bight, *J. Foraminiferal Res.*, *21*, 347–363.
Spero, H. J., K. M. Mielke, E. M. Kalve, D. W. Lea, and D. K. Pak (2003), Multispecies approach to reconstructing eastern equatorial Pacific thermocline hydrography during the past 360 kyr, *Paleoceanography*, *18*(1), 1022, doi:10.1029/2002PA000814.
Steinhardt, J., C. Cléroux, J. Ullgren, L. de Nooijer, J. V. Durgadoo, G.-J. Brummer, and G.-J. Reichart (2014), Anti-cyclonic eddy imprint on calcite geochemistry of several planktonic foraminiferal species in the Mozambique Channel, *Mar. Micropaleontol.*, *113*, 20–33, doi:10.1016/j.marmicro.2014.09.001.
Takayanagi, Y., N. Niitsuma, and T. Sakai (1968), Wall microstructure of *Globorotalia truncatulinoides* (d'Orbigny), *Sci. Rep. Tohoku Univ.*, *40*(2), 141–170.
Tunheng, A., and T. Hirata (2004), Development of signal smoothing device for precise elemental analysis using laser ablation-ICP-mass spectrometry, *J. Anal. At. Spectrom.*, *19*(7), 932–934, doi:10.1039/B402493A.
Urey, H. C., H. A. Lowenstam, S. Epstein, and C. R. McKinney (1951), Measurement of paleotemperatures and temperatures of the Upper Cretaceous of England, Denmark, and the southeastern United States, *Geol. Soc. Am. Bull.*, *62*(4), 399–416.
Van Raden, U. J., J. Groeneveld, M. Raitzsch, and M. Kucera (2011), Mg/Ca in the planktonic foraminifera *Globorotalia inflata* and *Globigerinoides bulloides* from Western Mediterranean plankton tow and core top samples, *Mar. Micropaleontol.*, *78*(3–4), 101–112, doi:10.1016/j.marmicro.2010.11.002.
Vetter, L., R. Kozdon, J. W. Valley, C. I. Mora, and H. J. Spero (2014), SIMS measurements of intrashell δ^{13}C in the cultured planktic foraminifer *Orbulina universa*, *Geochim. Cosmochim. Acta*, *139*, 527–539, doi:10.1016/j.gca.2014.04.049.
Vincent, E., and W. Berger (1981), Planktonic foraminifera and their use in paleoceanography, *The Sea*, *7*, 1025–1119.
Watkins, J. M., A. C. Mix, and J. Wilson (1996), Living planktic foraminifera: Tracers of circulation and productivity regimes in the central equatorial Pacific, *Deep Sea Res., Part II*, *43*, 1257–1282.
Weiner, S., and P. M. Dove (2003), An overview of biomineralization processes and the problem of the vital effect, *Rev. Mineral. Geochem.*, *54*(1), 1–29.
Wejnert, K. E., R. C. Thunell, and Y. Astor (2013), Comparison of species-specific oxygen isotope paleotemperature equations: Sensitivity analysis using planktonic foraminifera from the Cariaco Basin, Venezuela, *Mar. Micropaleontol.*, *101*, 76–88, doi:10.1016/j.marmicro.2013.03.001.
Wilke, I., T. Bickert, and F. J. Peeters (2006), The influence of seawater carbonate ion concentration [CO_3^{2-}] on the stable carbon isotope composition of the planktic foraminifera species *Globorotalia inflata*, *Mar. Micropaleontol.*, *58*(4), 243–258.
Wilke, I., H. Meggers, and T. Bickert (2009), Depth habitats and seasonal distributions of recent planktic foraminifers in the Canary Islands region (29°N) based on oxygen isotopes, *Deep Sea Res., Part I*, *56*, 89–106, doi:10.1016/j.dsr.2008.08.001.
Wit, J. C., G. J. Reichart, S. J. A. Jung, and D. Kroon (2010), Approaches to unravel seasonality in sea surface temperatures using paired single-specimen foraminiferal δ^{18}O and Mg/Ca analyses, *Paleoceanography*, *25*, PA4220, doi:10.1029/2009pa001857.
Zeebe, R. E., J. Bijma, B. Hönisch, A. Sanyal, H. J. Spero, and D. A. Wolf-Gladrow (2008), Vital effects and beyond: a modelling perspective on developing palaeoceanographical proxy relationships in foraminifera, Special Publications, *303*(1), 45–58, Geol. Soc., London, U. K.